Chapter 2

Theoretical Treatment of Organometallic Compounds

During the last years, commercially availability or free accessibility of often friendly-made and graphics-oriented program packages has caused a dramatic change in attitudes towards theory among organometallic chemists. In this regard, it is interesting to note that the 1998 Nobel Prize in Chemistry was awarded to John A. Pople and Walter Khon for their contribution to spread computational chemistry. However, the results of calculations need to be viewed cautiously, since their reliability is strongly influenced by the employed method and its intrinsic features. The use of computational methods as a black box *may lead to artifacts. Thus, the intention of the present chapter is to briefly describe the main features of theoretical methods that are currently in use for studying organometallic compounds, taking special emphasis in those methods used in this thesis. In addition, we try to provide the non-experienced readers with some guidance on how to use, understand, and assess the limitations on the calculations of these studies. Description will be done with minimal mathematical survey.*

Nowadays, there are a wide and expanding variety of methods in computational chemistry, ranging from the very approximate to the very precise.[1] *Computational methods are largely applied in the field of transition metal and organometallic chemistry. Recently, several publications have reviewed the theoretical studies that have been carried out in this field, and have reassessed the reliability of the methods.*[2-4] *The early stages of computational organometallic chemistry were marked by qualitative molecular orbital (MO) theory based on extended Hückel (EH) calculations. These studies, although of a qualitative nature, founded the theoretical basis of organometallic chemistry. Later on, the application of ab initio quantum chemistry methods, either based on the Hartree-Fock (HF) theory or on density functional theory (DFT) began to yield semiquantitative results. However, more advanced methods were still required to get reliable results. For transition metal compounds, it is generally accepted that*

minimal approaches require incorporating dynamic correlation (in HF theory) and the use of non-local functional (in DFT theory). In the 1990s, the development of faster and cheaper computers, commercial programs incorporating latest methods, effective potentials replacing core electrons of transition metals allowed performance of accurate calculations. Thus, more advanced HF based methods, such as Møller-Plesset perturbation theory, configuration interaction, or coupled cluster theory became available for systems with simplified ligands. Another major impact in computational chemistry came from the widespread acceptance of density functional methods, which yielded reliable structures and energies with simpler computations. Currently, the use of hybrid quantum mechanics/ molecular mechanics (QM/MM) methods to model steric effects of bulky ligands is becoming more and more popular. Also, some methods for analyzing the electronic structure such as the natural bond population (NBO) analysis or the Bader's analysis have been developed during last years.

The theoretical study of organometallic compounds have to deal with many problems such as the correct and accurate description of the multiple molecular properties and isomers, the diversity of oxidation states, the size of the ligands, the solvent effects, the relativistic effects that come into play, or the competition of reaction pathways. Thus, and despite of the great effort made in the theoretical organometallic field, an accurate theoretical treatment of these compound remains a challenge due to their versatile nature.

2.1 QUALITATIVE MOLECULAR ORBITAL THEORY

The first impact of theoretical chemistry on organometallic chemistry appeared mostly in the form of qualitative molecular orbital (MO) theory. Hoffmann and coworkers pioneered in the application of theoretical tools to this field, with approaches based on Extended Hückel (EH) calculations.[5] Unlike sophisticated electronic methods, qualitative methods are unable to provide accurate results, but they may be useful for gaining insight into electronic structure and reactivity. These methods are concerned for "how" rather than for "how much" of organometallic chemistry. Thus, results are easier to rationalize, and therefore it becomes easier to apply the findings to other similar systems. Furthermore, they provide a link between theoretical chemistry and many concepts used by experimentalists.

Qualitative MO theory considers the individual interactions between the orbitals of reacting entities.[6] In general, two interacting orbitals generate two new orbitals, one with lower energy and the other with higher energy. The most important interactions take place between orbitals that are closest in energy and have a large overlap. When these interactions involve two electrons they are of stabilizing nature, while if four electrons are involved they are of destabilizing nature. Finally, another feature to be considered is the polarization of an orbital that results from the mixing of orbitals.

The Extended Hückel (EH) calculations[5] only consider the valence electrons and involve parameterization that converts them in non-iterative methods. Also, the one particle nature of Hückel theory allows expressing the total energy as the sum of orbital energies. The simplicity of these methods makes them suitable for the qualitative treatment of orbital interactions. However, this does not mean that it is restricted to EH calculations, more elaborate calculations can also be used. From these calculations one can construct orbital interaction diagrams and orbital correlation diagrams. Both sorts of diagrams are convenient tools when dealing with organometallic reactivity. They can be used to underline the critical features of any generic reaction. Moreover, by using the fragment molecular orbital (FMO) analysis[6] and the isolobal analogy concept[7] one can attempt to predict relative reactivities based on the properties of the reactants.

2.2 NONEMPIRICAL METHODS

Qualitative molecular orbital methods can give useful answers about transition metal chemistry, but in most cases, they cannot provide precise determination of structures and energies. In contrast, accurate quantum mechanical methods can yield reliable results for molecules of reasonable size in gas phase. Thus, if we are interested in describing the electron distribution in detail, there is no substitute to quantum mechanics. Both, standard ab initio (Hartree-Fock based) methods and the density functional theory (DFT) methods are widely used in computational organometallic chemistry.

The theoretical study of the organometallic reactivity requires of the determination of the geometries and the computation of the energies of the reactives, products, all relevant intermediates and transition states. In other words, it concerns with the localization of the stationary points of the Potential Energy Surface and their energy evaluation. Optimization of geometries is usually done in all degrees of freedom through gradient techniques[8]. In the procedure all degrees of freedom are varied simultaneously until the gradient (first derivatives) of the energy is zero. This means that reactives, products, intermediates and transition states are stationary points, in which, the forces acting on the system are zero.

The characterization of the stationary points involves the differentiation between the local minima (intermediates, reactants, products) and the saddle points (transition states). To do that the matrix of the second derivatives of the energy with respect to internal coordinates (Hessian matrix) must be computed. The Hessian matrix gives information about the curvature of the surface at the stationary point. In the case of local minima all the eigenvalues of the Hessian matrix are positives, indicating that the energy is minimum in all directions. On the other hand, in saddle points, there is one and only one negative eigenvalue, indicating the energy is minimum in all directions but one. The negative eigenvalue of a transition state corresponds to an imaginary vibrational frequency, whose normal mode should be examined in order to check whether the transition state connects the right reactant and the right product. In some instances, it may not be straightforward whether the appropriate transition state has been determined and the intrinsic reaction coordinate (IRC) should be calculated.[9] The IRC follows the reaction path from the transition state to the two connected local minima.

Once the geometries have been optimized, the energy can be computed. Due to the rather large size of transition metal complexes it is not unusual to perform energy calculation and geometry optimization at different level of computational accuracy. The geometry is obtained at a lower level and the energy is computed at

a much higher level. It has been shown over the years that this is generally a safe procedure, although it may in some instances lead to artifacts.[10]

2.2.1 Standard Ab Initio Methods

The aim of ab initio (Latin: "from the beginning") calculations is finding an approximate solution to the non-relativistic time independent Schrödinger equation.[11]

$$\hat{H}\Psi = E\Psi \qquad \textbf{(2.1)}$$

Approximations are introduced in the Hamiltonian ($\hat{H}$) and in the wave function (Ψ). Since nuclei are much heavier than electrons, they move more slowly. Thus, a good approximation can be to consider the electrons in a molecule to be moving in the field of fixed nuclei. The Born-Oppenheimer approximation leaves out of the equation nuclear motion and only the electronic Schrödinger equation is solved. Its solution is the central problem of quantum chemistry. The wave function is expressed in terms of products of one-electron function, the spin-orbitals, which are itself the product of a spatial function (molecular orbital) and a spin function. The simplest wavefunction is a single Slater determinant for which the variational optimization of the spin-orbitals is carried out in a self-consistent field (SCF) manner through the canonical Hartree-Fock (HF) equations.[12] Within the LCAO-MO procedure molecular orbitals are obtained as linear combination of atomic orbitals (basis functions).[13] In other words, spin-orbitals are expanded in a basis function centered on the atoms. Thus, the larger the basis set is, the more accurate the determination of the energy will be. Another approximation usually made when dealing with transition metal complexes is the use of effective core potentials (ECP).[14] In this approximation only the valence electrons of the metal are treated explicitly, and the action of the inner shell electrons on the balance electrons is described by an ECP.

The HF approximation does not account for electron correlation, which is defined as the difference in energy between the HF and the exact energy.[15] In the single determinant (or single configuration) HF picture the real electron-electron interaction is replaced by an average interaction. This implies that the movement of electrons in order to avoid instantaneous electronic repulsions is not considered. Furthermore, the contribution of near excited states, i. e., the contribution of more than one electronic configuration to the ground state is neglected. These two missing effects are called, respectively, dynamic and non-dynamic electron

correlation. However, there is no rigorous way to separate them. For transition metal complexes, nowadays, it is generally accepted that minimal approaches require introduction of correlation in order to get reliable results. To handle the electron correlation problem, a multideterminant description of the wave function Ψ must be resorted. The wave function is expanded over a basis of determinants (or configurations), and the Schrödinger equation is solved either variationally or perturbatively.

A variety of post-HF methods, introducing electron correlation in different ways, are available. The variational treatment is performed in the configuration interaction (CI) methods,[16] and in the multiconfigurational self-consistent field (MCSCF) methods[17] such as the CASSCF method.[18] Correlation can also be introduced perturbationally; the Møller-Plesset (MP) method[19] is one of the most popular methods. The perturbation can be carried out to various orders (MP2, MP3, MP4, etc.), being the fourth order the limit for current computational resources. Other treatments are also available to include correlation effects, being very precise but highly computationally demanding: the multireference configuration interaction (MRCI) methods[20] and the coupled cluster (CC) methods.[21] Nowadays, the CCSD(T) method is generally consider being the state of the art for transition metal complexes, i. e., the limit of what can be calculated for current computational affordability. In this coupled cluster method, the operator acting on HF reference wave function generates single and double excitations, while triple excitations are perturbationally estimated.

2.2.2 Density Functional Theory Methods

Another way to introduce electron correlation is through the use of methods based on the Density Functional Theory (DFT).[22] Unlike the ab initio methods mentioned above, no attempt is made to solve directly the Schrödinger equation. Instead, the energy is expressed as a functional of the electron density. In other words, the interacting system is described via its electron density (ρ) and not via its wave function (Ψ). Density functional methods have been proved to be very successful since the 1990s, especially in organometallic chemistry.[23] The main attraction lies in their ability to treat even rather large molecular systems with comparable accuracy but faster, and thus less computationally demanding, than by standard wave function based methods. Furthermore, DFT methods are currently implemented in most of commercial ab inito program packages. Thus, as Professor Ernest R. Davidson states in the editorial of the 2000 *Chemical Reviews* issue on Computational Transition Metal Chemistry:[2] "nowadays, *computational transition metal chemistry is almost synonymous with DFT for medium-sized molecules".*

DFT methods have been developed on the basis of the Hohenberg-Kohn theorem[24] and the Kohn-Sham approximation.[25] The Hohenberg-Kohn (HK) theorem states that all-ground state properties of a system are functions of the electron charge density (ρ), i. e., it exists a one-to-one correspondence between the ρ of the system and the energy. Today, DFT is put into practice almost exclusively via the Kohn-Sham (KS) approximation, which allows optimizing the energy by solving a set of one-electron equations, the KS orbitals. To the non-specialists, the K-S scheme resembles that of HF method, and the KS orbitals can be also expressed as a linear combination of atomic orbitals. These theorems enable us to write the total electron energy as a function of the electron density.

$$E_{\mathrm{DFT}}(\rho) = T_{\mathrm{S}}(\rho) + E_{ne}(\rho) + E_{\mathrm{J}}(\rho) + E_{\mathrm{XC}}(\rho) \quad \textbf{(2.2)}$$

where T_S is the non-interacting kinetic energy, E_{ne} includes terms describing the potential energy of the nuclear-electron attraction, E_J is the electron-electron repulsion, and E_{XC} is the exchange-correlation term, in which the electron correlation effects and the remaining part of the electron-electron interactions are included. The problem of DFT methods is that the functional connecting the electron density with the energy is unknown. Thus, the goal of DFT methods is to design functionals connecting these two quantities.

In the previous equation, mathematical expressions of the first three components of the energy are well known, however, for the exchange-correlation term (E_{XC}) some approximations must be made. The early way to obtain this contribution to energy uses the so-called local density approximation (LDA), in which the E_{XC} term only depends on the local electron-density value. It assumes that the charge density varies slowly throughout the molecule so that the density can be treated as an uniform electron gas. The fit by Vosko, Wilk, Nusair (VWN)[26] has been one of the most commonly used in the chemical literature. The LDA approximation generally gives good results for the determination of structural features of the system, as well as for vibrational frequencies and dipole moments. However, it usually overestimates the binding energies. This can be significantly improved by adding gradient corrections to both the exchange and correlation functionals, through terms that involve the gradient of the density. It has been proposed several functionals belonging to this class of methods, generalized gradient approximation (GGA). Outstanding examples are the exchange functional proposed by Becke in 1988,[27] correlation functional proposed by Perdew in 1991,[28] or the correlation functional proposed by Lee, Yang and Parr.[29] They are usually noted with the initials of the authors' surname followed by the year in

which the model was published. Today program packages allow combining the different exchange and correlation functionals when performing a calculation.

Another approach that has been quite successful is the so-called hybrid functional, which deviates somewhat from pure DFT methods. Hybrid methods mix the standard Kohn-Sham form of the exchange energy with the Hartree-Fock exchange (non-local single-determinant exchange). Indeed, in many aspects, hybrid methods are considered to be the most accurate DFT procedures available at the present. Currently the most popular hybrid method is the semi-empirical B3LYP scheme (Becke-exchange-3-parameter-Lee-Yang-Parr-correlation). It owes its origins to a proposal by Becke[30] for a parameterized hybrid approximation involving the Perdew correlation functional,[28] which lately was substituted by the LYP correlation functional.[29]

Despite the advantages of DFT methods respect to standard ab initio methods, there are, however, several drawbacks. Unlike standard ab initio approaches, DFT methods do not provide a prescription how to calculate truth. The exact form of the universal energy density functional relating electron density to energy is unknown, and there is no general way to systematically improve it besides trying new ones and judging their quality by the results. Moreover, DFT is in principle only applicable to the ground state, and its extension to excited states is no obvious. However, approaches such those based on time-dependent DFT have recently begun to be applied to describe excited state properties in transition metal complexes.[31] Other strategies, consisting of formulation of the energy as the weighted sum of single determinant energies, have been also proposed to access multiplet splittings.[32]

2.3 HYBRID QM/MM METHODS

Both, standard ab initio and DFT methods, are restricted to medium size systems, consisting typically of one or two transition metals and of ligand with total number of lighter atoms not exceeding 50. Thus, despite of the growing computer power, these methods are often prohibitive to the study of large systems with bulky ligands. An approach that has been extensively applied is the use of model systems. A typical example is the replacement of any real-world phosphine by the simplified PH_3. The significance of theoretical studies using model systems is not as limited as one could expect, because the metal-ligand interactions remain well reproduced. However, there are a number of chemical features that depend on the specific nature of the ligand, and cannot be assessed by these model system calculations. Some approaches, especially those based on hybrid quantum

mechanics/molecular mechanics (QM/MM) methods, are beginning to fulfil the gap between real-world complexes and computer models.

One possible way to introduce bulk ligand effects is the use of semiempirical methods especially tailored for transition metal systems. In this respect, promising results have been obtained with PM3(tm) method,[33a] nevertheless it have been found that its reliability depends on the particular cases.[33b] Another major way to study large transition metal systems is the use of pure molecular mechanics (MM) calculations.[34] Molecular mechanics is a simple, empirical *ball-and-spring* model, which have been widely used in organic chemistry. The size of the balls (atoms) and the rigidity of the springs (bonds) are determined empirically from experimental data. In organometallic chemistry, there is a much larger variety of elements and binding modes than in organic chemistry. Therefore, parameterization is much more complicated, and the development of a specific force field for each compound, or family of compounds is required. Approaches have been also proposed involving QM calculations on model systems to fit MM parameters.[35]

In the hybrid QM/MM methods the molecular system is divided in different regions, and each of them is treated at different computational level. In transition metal complexes, the active region (metal center) is treated with an accurate quantum mechanic (QM) method, and the remainder system (bulk of the ligands) can be treated with a much more affordable molecular mechanics (MM) approach. However, the QM/MM partition is not always straightforward, and chemical knowledge is often the main guiding line for this choice.

Several QM/MM methods have been described in the literature.[36] Most of them have been developed to introduce solvation effects, with especial focus on biochemical systems. In this thesis, the study of a homogeneous catalytic process, the hydroformylation, has been performed by means of one of these QM/MM methods, the Integrated Molecular Orbital Molecular Mechanics (IMOMM) method.[37] The main difference between this method and the majority of other available QM/MM methods is related to the handling of the interaction between QM and MM regions. IMOMM method has been the starting point for other QM/MM methodological developments[38] such as the IMOMO[38a] and the ONIOM[38b] methods. The IMOMO method is the extension of the method to the use of two different-quality QM descriptions. The ONIOM method is essentially a generalization that encompasses both the IMOMM and IMOMO methods, allowing using more than two layers. The IMOMM and its derived forms have been so far the most widely applied to transition metal systems.

In principle, in any hybrid QM/MM method the total energy of the whole system can be expressed as:

$$E_{TOT}(QM,MM) = E_{QM}(QM) + E_{MM}(MM) + E_{INTERACTION}(QM/MM) \quad \textbf{(2.3)}$$

where the subscript labels refer to the type of calculation and the labels in parenthesis correspond to the region under study. The E_{QM}(QM) and E_{MM}(MM) terms are simply the pure QM and MM calculations of the corresponding regions. The other term correspond to the evaluation of the interaction energy between both regions. In principle, the interaction energy can be evaluated by both the QM and the MM methods and, consequently, can be divided in two new energy terms, E_{QM}(QM/MM) and E_{MM}(QM/MM). Computational approaches differ by the way these two terms are calculated. The E_{QM}(QM/MM) term is usually critical in solvation problems, because it accounts for the effect of atoms in MM part on the QM energy of the system, i. e., the effect of the solvent in the quantum mechanics properties of the solute. In the case of transition metal complexes, this term accounts mainly for the electronic effects of the ligand substituents on the metal center. The E_{MM}(QM/MM) term accounts for the geometrical constrains of metal center (QM) on the geometry of the ligands (MM). This means that is mostly related to the steric effects of the ligand substituents.

2.3.1 The IMOMM Method

The IMOMM and derived methods involve a full multistep optimization. This means that the geometry corresponds neither to the optimal QM arrangement nor to the optimal MM arrangement, but a compromise between both. This treatment is different from simpler one-step (QM then MM) methods, where the MM geometry is optimized on a frozen QM geometry. Another characteristic of the IMOMM method is that atoms in the MM region do not have a direct effect on the QM region, except through the distortions they induce in the geometry. In other words, this scheme simply neglects the E_{QM}(QM/MM) term, and only steric effects of atoms in MM region are included. On one hand this supposes the introduction of an error because the electronic contributions of MM atoms are left out. On the other hand, this allows a straightforward separation between electronic and steric effects. In order to introduce part of the electronic effects, other QM/MM approaches have proposed the use of point charges[36f] or, in a more elaborate scheme, localized orbitals.[36g] Within the IMOMM scheme, the natural solution is to expand the QM region in order to include all significant electronic effects.

Applications have concentrated mostly in transition metal complexes, especially in those areas where the calculation of simplified models could not

account for the experimental complexity. Most of the work has been made in homogeneous catalysis[39] and in structural issues associated with steric effects,[40] although not exclusively. Also these methods have been applied to the study of bioinorganic systems,[41] zeolites,[42] and heterogeneous catalysis.[43]

2.4 ANALYSIS OF THE ELECTRONIC STRUCTURE

The last decades have not only witnessed progress in computational chemistry methods for calculating measurable properties of molecules, but also theoretical methods have been developed to analyze the calculated electronic structure. In this section we give a short outline of the essential features of two methods, which are now widely used for analyzing the chemical bonds in organometallic compounds. These are the atoms in molecules (AIM) method suggested by Bader,[44] and the natural bond orbital (NBO) method developed by Weinhold,[45] both have been used along the thesis.

2.4.1 Bader Analysis: Information from the Electron Density

The Bader analysis of electron density is based on the atoms in molecules (AIM) theory.[44] It provides a set of practical tools for analyzing the electronic structure of a molecule, which is based on the electron density distribution. An attractive feature of the AIM model is that electron density distribution is an observable quantity. Therefore, Bader's analysis can be performed either on experimental (X-ray) and theoretical electron density.

The central idea of AIM theory is that the topology of electron density $\rho(r)$ contains information about the bonding situation, which can be elucidated through mathematical analysis of $\rho(r)$. The topological analysis of any scalar function, such as $\rho(r)$, consists of determination of the points in which first derivatives ($\nabla\rho(r)$) are zero. When dealing with electron density, these points are called critical points (cp) and they can be classified according the principle curvatures (eigenvalues) of the associated second derivatives of $\rho(r)$ in three-dimensional space. The position of atomic nucleus is defined as a cp in which all the curvatures of $\rho(r)$ are negative. It is a maximum of local density labeled as a (3, -3) point. A bond critical point (bcp) has two negative curvatures (maximum) and one positive curvature (minimum), and is labeled as (3, -1) point. The trajectory that belongs to the positive curvature is the bond path connecting the two bonded atoms. Two other types of critical points can be defined, the ring (3, +1) and the cage (3, +3) critical points.

It is not always straightforward to determine whether two atoms are bonded or not. However, according to Bader's AIM theory, the necessary and sufficient condition for two atoms to be bonded is the presence of a bond cp between them. Moreover, the values of $\rho(r)$, Laplacian ($\nabla^2\rho(r)$), and ellipticity (ε) at the bcp's can be used to gauge the variation of electron density and bonding nature which occur upon structural changes. The value of $\rho(r)$ at the bcp's can be considered a measure of the bond strength; thus, the larger the $\rho(r)$, the stronger the bond. It have been observed that large and negative values of Laplacian are indicative of shared interactions, characterized by a large accumulation of charge between the nuclei. On the other hand, for closed-shell interactions (ionic bonds, hydrogen bonds, and van der Waals interactions) Laplacian is low and positive. Also, the value of ε provides a measure for the π character of a bond.

Analogously, the topological analysis can be also performed on the Laplacian of electron density ($\nabla^2\rho(r)$). The analysis is usually carried out on $-\nabla^2\rho(r)$ function because main interest lies on charge concentration, which corresponds to negative areas of Laplacian. This function gives important information on the nature of the chemical interaction between atoms. Representation of Laplacian maps can serve also to reveal the shell structure of atoms in molecules. Besides it, local maxima of $-\nabla^2\rho(r)$ can be associated also with the Lewis idea of localized electron pairs and gives a physical basis for the Valence Shell Electron Pair Repulsion (VSEPR) model.

2.4.2 Natural Bond Orbital Method

Another theoretical tool for analyzing the electronic structure, which is not based on electron density but rather on orbitals, is the Natural Bond Orbital (NBO) method.[45] This and other quantum chemical partitioning schemes concern with the distribution of electrons into atomic and molecular orbitals, and thereby with the derivation of atomic charges and molecular bonds. Two analysis derive from NBO method; the NBO analysis for the assignment of molecular bonds and the Natural Population Analysis (NPA) for assignment of atomic charges. The NBO method merged as an alternative to the extensively used Mulliken population analysis.[46] On the one hand, it overcomes some of its limitations, namely the unphysical results when non-covalent bonds are considered and the basis set dependence. The NBO method is quite robust toward changing the basis set. On the other hand, it shares some of the most appealing features of the Mulliken method, like the low computer cost and the general applicability to any wavefunction.

The idea in NBO method is to use the one-electron density matrix for defining the shape of atomic orbital in the molecular environment. The method takes as

reference the atomic ground state and assigns as valence space all the orbitals that are in fully or partially occupied shells, and as Rydgberg space all the orbitals that are in empty space. The procedure involves a different treatment for the two sets of orbitals though the application of a weighting factor, which favors the minimal basis set and ensures stability toward basis set enlargement.

REFERENCES

General.

1. Jensen, F. *Introduction to Computational Chemistry*, Wiley, Chichester, 1999.
2. Thematic issue 100 of *Chem. Rev.* **2000**, p 351.
3. Brown, J. M.; Hofmann, P. (eds.) *Topics in Organometallic Chemistry: Organometallic Bonding and Reactivity. Fundamental Studies*, (vol. 4), Springer, Heidelberg, 1999.
4. Cundari, T. R. (ed.) *Computational Organometallic Chemistry*, Marcel Dekker, New York, 2001.

Qualitative MO Methods.

5. Hoffmann, R. *J. Chem. Phys.* **1963**, *39*, 1397.
6. Albright, T. A.; Burdett, J. K.; Whangbo, M. H. *Orbital Interactions in Chemistry*; Wiley: New York, 1985.
7. Hoffmann, R. *Angew. Chem., Int. Ed.* **1982**, *21*, 711.

Nonempirical Techniques

8. (a) Schlegel, H. B. in: *Ab initio Methods in Quantum Chemistry I*, Lawley Ed. John Wiley & Sons; New York, 1987. (b) Pulay, P. *Adv. Chem. Phys.* **1987**, *69*, 241. (c) Helgaker, T.; Jorgensen, P. *Adv. Quant. Chem.* **1988**, *19*, 183. (d) Schlick, T. in: *Reviews in Computational Chemistry*, Vol. 3, Lipkowitz, K B.; Boyd, D. B., Eds.; VCH: New York, 1992, p 1. (e) MacKee, M. L.; Page, M. in: *Reviews in Computational Chemistry*, Vol. 4, Lipkowitz, K B.; Boyd, D. B., Eds.; VCH: New York, 1993, p 35.
9. (a) Fuckui, K. *Acc. Chem. Res.* **1981**, *14*, 363. (b) Gonzalez, C.; Schlegel, H. B. *J. Phys. Chem.* **1990**, *94*, 5523.
10. (a) Müller, K.; *Angew. Chem., Int. Ed. Engl.* **1980**, *19*, 1. (b) Ishida, K.; Morokuma, K.; Komornicki, A. *J. Chem. Phys.* **1977**, *66*, 2153.

Standard Ab Initio Methods.

11. Szabo, A.; Ostlund, N. S. *Modern Quantum Chemistry*, 1st Edition revised, McGraw-Hill, New York, 1989.
12. (a) Hartree, D.R. *Proc. Cambridge Phil. Soc.* **1928**, *24*, 89. (b) Fock, Z. *Z. Physik* **1939**, *61*, 126.
13. Roothan, C.C. *Rev. Mod. Phys.* **1951**, *23*, 69.
14. (a) Krauss, M.; Stevens, W. J. *Ann. Rev. Phys. Chem.* **1984**, *35*, 357. (b) Durand, P.; Malrieu, J. P. *Adv. Chem. Phys.* **1987**, *67*, 321.

15. Löwdin, P.O. *Adv. Chem. Phys.* **1959**, *2*, 1207.
16. (a) Shavitt, I. *Methods of Electronic Structure Theory*, Schaefer III Ed., Plenum Press, New York, 1977. (b) Roos, B. *Chem. Phys. Lett.* **1972**, *15*, 152. (c) Knowles, P.J.; Handy, N.C.; *Chem. Phys. Lett.* **1984**, *111,* 315.
17. Olsen, J.; Yeager, D. L.; Jorgensen, P. *Adv. Chem. Phys.* **1983**, *54*, 1.
18. Roos, B. O.; Taylor, P. R.; Sieghban, P. I. M. *Chem. Phys.* **1980**, *48*, 157.
19. Möller, C. Plesset, M.S. *Phys. Rev.* **1934**, *46*, 618.
20. (a) Werner H. –J.; Knowles, P. J. *J. Chem. Phys.* **1988**, *89*, 5803. (b) Werner H. –J.; Knowles, P. J. *Chem. Phys. Lett.* **1988**, *145*, 514.
21. Cizek, J. *J. Chem. Phys.* **1966**, *45,* 4256.

Density Functional Theory (DFT).

22. Parr, R. G.; Yang, W. *Denstity Functional Theory of Atoms and Molecules*, Oxford University Press, Oxford, 1989.
23. (a) Ziegler, T. *Chem. Rev.* **1991**, *91*, 649. (b) Ziegler, T. *Can. J. Chem.* **1995**, *73*, 743. (c) Görling, A.; Trickey, S. B.; Gisdakis, P.; Rösch, N. in *Topics in Organometallic Chemistry: Organometallic Bonding and Reactivity. Fundamental Studies*, Brown, J. M.; Hofmann, P., Eds., Springer, Germany, 1999, p. 109.
24. Hohenberg, P.; Kohn, W. *Phys. Rev. B* **1964**, *136*, 864.
25. Kohn, W. Sham, L. J. *Phys. Rev. A* **1965**, *140*, 1133.
26. Vosko, S. J.; Wilk, L.; Nusair, M. *Can. J. Phys.* **1980**, *58*, 1200.
27. (a) Becke, A. D. *Phys. Rev. B* **1986**, *33*, 8822. (b) Becke, A. D. *Phys. Rev. A* **1988**, *38*, 3098.
28. Perdew, J. P. *Electronic Structure of Solids '91*, Ziesche, P.; Eschring, H. Eds., Akademie, Berlin, 1991.
29. Lee, C.; Yang, W.; Parr, R. G. *Phys. Rev. B* **1988**, *37*, 785.
30. Becke, A. D.; *J. Chem. Phys.* **1993**, *98*, 5648.
31. For some recent references: (a) Boulet, P.; Buchs, M.; Chermette, H.; Daul, C.; Gilardoni, F.; Rogemond, F.; Schläpfer, C. W.; Weber, J. *J. Phys. Chem. A* **2000**, *105*, 8999. (b) Full, J.; González, L.; Daniel, Ch. *J. Phys. Chem. A* **2000**, *105*, 184. (c) Adamo, C.; Barone, V. *Theo. Chem. Acc.* **2000**, *105*, 169. (d) Rosa, A.; Baerends, E. J.; van Gisbergen, S. J. A.; van Lenthe, E.; Gooeneveld, J. A.; Snijders, J. G. *J. Am. Chem. Soc.* **1999**, *121*, 10356.
32. (a) Daul, C. *Int. J. Quantum Chem.* **1994**, *52*, 867. (b) Dickson, R.; Ziegler, T. *Int. J. Quantum Chem.* **1996**, *58*, 681.

Hybrid QM/MM Methods.

33. (a) Børve, K. J.; Jensen, V. R.; Karlsen, T.; Støvneng, J. A.; Swang, O. *J. Mol. Mod.* 1997, *3*, 193. (b) Bosque, R.; Maseras, F. *J. Comp. Chem.* **2000**, *21*, 562.
34. Comba, P.; Hambley, T. W. *Molecular Modeling of Inorganic Compounds*, VCH, Weinheim, 1995.
35. (a) Cundari, T. R.; Sisterhen, L. L.; Stylianopoulos, C. *Inorg. Chem.* **1997**, *36*, 4029. (b) Cundari, T. R.; Saunders, L.; Sisterhen, L. L. *J. Chem. Phys. A* **1998**, *102*, 997. (c) Norrby, P. –O. *J. Mol. Struct. (TEOCHEM)* **2000**, *506*, 9.
36. (a) Warshel, A.; Levitt, *J. Mol. Biol.* **1976**, *103*, 227. (b) Singh, U. C.; Kollman, P. A. *J. Comput. Chem.* **1986**, *7*, 119. (c) Field, M. H.; Bash, P. A.; Karplus, M. *J. Compt. Chem.* **1990**, *11*, 700. (d) Gao, J. *Acc. Chem. Res.* **1996**, *29*, 119. (e) Gao, J. *Rev. Comput. Chem.* **1996**, *7*, 119. (f) Bakowies, D.; Thiel, W. *J. Phys. Chem.* **1996**, *100*, 10580. (g) Tuñon, I.; Martins-Costa, M. T. C.; Millot, C.; Ruiz-López, M. F. Rivail, J. –L. *J. Comput. Chem.* **1996**, *17*, 19. (h) Monard, G.; Merz, K. M. *Acc. Chem. Res.* **1999**, *32*, 904. (i) Zhang, Y.; Liu, H.; Yang, W. *J. Chem. Phys.* **2000**, *112*, 3483. (j) Gogonea, V.; Westerhoff, L.M.; Merz, K.M. *J. Chem. Phys.* **2000**, *113*, 14.
37. (a) Maseras, F.; Morokuma, K. *J Comput Chem*. **1995**, *16*, 1170. (b) Maseras, F.; *Chem.Commun*. **2000**, 1821.
38. (a) Humbel, , S.; Sieber, S.; Morokuma, K. *J. Chem. Phys.* **1996**, *105*, 1959. (b) Dapprich, S.; Komáromi, I.; Byun, K. S.; Morokuma, K.; Frisch, M. J. *J. Mol. Struct. (THEOCHEM)* **1999**, *461*, 1. (c) Woo, T. K.; Cavallo, L.; Ziegler, T. *Theor. Chem. Acc.* **1997**, *119*, 6177. (d) Shoemaker, J. R.; Burggraf, L. W.; Gordon, M. S. *J. Phys. Chem. A* **1999**, *103*, 3245.
39. For some recent references, see: (a) Ujaque, G.; Maseras, F.; Lledós, A. *J. Am. Chem. Soc.* **1999**, *121*, 1317. (b) Vázquez, J.; Pericàs, M. A.; Maseras, F.; Lledós, A. *J. Org. Chem.* **2000**, *65*, 7303. (c) Feldgus, S.; Landis, C. R. *J. Am. Chem. Soc.* **2000**, *122*, 12714. (d) Feldgus, S.; Landis, C. R. *Organometallics* **2001**, *20*, 2374. (e) Goldfuss, B.; Steigelmann, M.; Khan, S. I.; Houk, K. N. *J. Org. Chem.* **2000**, *65*, 77. (f) Cavallo, L.; Solà, M. *J. Am. Chem. Soc.* **2001**, *123*, 123. (g) Milano, G.; Guerra, G.; Pellecchia, C.; Cavallo, L. *Organometallics*, **2000**, *19*, 1343. (h) Musaev, D. G.; Froese, R. D. J.; Morokuma, K. *Organometallics* **1998**, *17*, 1850.
40. (a) Barea, G.; Lledós, A.; Maseras, F.; Jean, Y. *Inorg. Chem.* **1998**, *37*, 3321. (b) Ujaque, G.; Cooper, A. C.; Maseras, F.; Eisenstein, O.; Caulton, K. G. *J. Am. Chem. Soc.* **1998**, *120*, 361.
41. (a) Marechal, J. -D; Barea, G.; Maseras, F.; Lledós, A.; Mouawad, L.; Perahia, D. *J. Comp. Chem.* **2000**, *21*, 282. (b) Torrent, M.; Vreven, T.; Musaev, D. G.; Morokuma, K.; Farkas, O.; Schelgel, H. B. *J. Am. Chem. Soc.* **2002**, *124*, 192.

42. (a) Rodríguez-Santiago, L.; Sierka, M.; Branchadell, V.; Sodupe, M.; Sauer, J. *J. Am. Chem. Soc.* **1998**, *120*, 1545. (b) Roggero, I.; Civalleri, B.; Ugliengo, P. *Chem. Phys. Lett.* **2001**, *341*, 625. (c) Sierka, M.; Sauer, J. *J. Phys. Chem. B* **2001**, *105*, 1603.
43. Lopez, N.; Pacchioni, G.; Maseras, F.; Illas, F. *Chem. Phys. Lett.*, **1998**, *294*, 611.

Analysis of Electron Structure.

44. (a) Bader, R. F. W. *Atoms in Molecules: A Quantum Theory*; Clarendon Press: Oxford, U. K., **1990**. (b) Bader, R. F. W. *Chem. Rev.* **1992**, *92*, 893.
45. Reed, A. E.; Curtiss, L. A.; Weinhold, F. *Chem. Rev.* **1988**, *88*, 899.
46. Mulliken, R. S. *J. Chem. Phys.* **1955**, *23*, 1833.

Chapter 3

Two- and Four-Electron-Alkyne Ligands: Consequences of the $\pi_{\perp} \rightarrow M$ Interaction

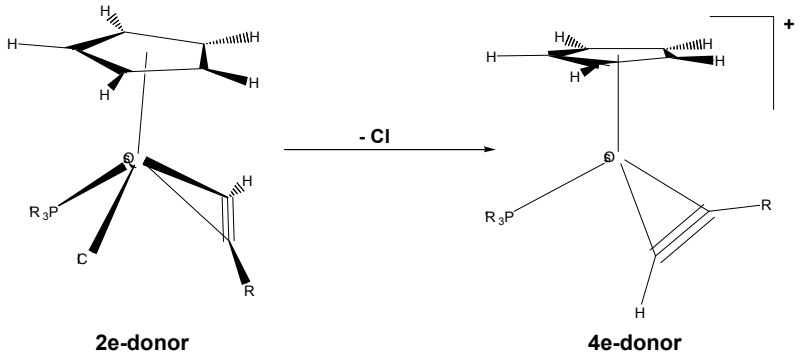

*The complexes Os(η^5-C_5H_5)Cl{η^2-HC≡CC(OH)R_2}(P^iPr_3) (R = Ph (**1a**), Me (**1b**)) react with $TlPF_6$ to give [Os(η^5-C_5H_5){η^2-HC≡CC(OH)R_2}(P^iPr_3)]PF_6 (R = Ph (**2a**), Me (**2b**)). The structures of **1a** and **2a** have been determined by X-ray diffraction. The comparative study of the data reveals a shortening of the OsC-(alkyne) distances on going from **1a** to **2a**, whereas the acetylenic bond length remains almost identical. Comparison of their ^1H and $^{13}C\{^1H\}$NMR spectra shows that the HC≡ proton resonances and the chemical shifts of the acetylenic carbon atoms of **2a** and **2b** are substantially shifted towards lower field than those of **1a** and **1b**.*

*DFT calculations were carried out on Os(η^5-C_5H_5)Cl(η^2-HC≡CR)(PH_3) (R = H (**A**), R = CH_3 ($\mathbf{A^{CH3}}$)) and [Os(η^5-C_5H_5)(η^2-HC≡CR)(PH_3)]$^+$ (R = H (**B**), R = CH_3 ($\mathbf{B^{CH3}}$)) model systems in order to study the differences in bonding nature of the two parent alkyne complexes, **1** and **2**. Calculations give geometries very close to the X-ray determined ones, and by using GIAO method we succeed in qualitatively reproducing the experimental ^1H and ^{13}C chemical shifts. Both structural and*

*spectroscopic changes can be explained by the participation of the acetylenic second π orbital ($\pi_\perp$) in the metal-alkyne bonding. On going from **1** to **2** or from **A** to **B**, the extraction of the chloride ligand transforms the two-electron donor alkyne ligand in a four-electron donor one, with both the $\pi_{||}$ and the $\pi_\perp$ orbitals donating to the metal, and stabilizing the otherwise 16-electron unsaturated complex **2**. Calculations also predict an increase of dissociation energies of the alkyne, and an enhancement in the energy of rotation of the alkyne, for complex **B**. Finally, the Bader's atoms in molecules (AIM) analysis shows that differences in coordination nature are also reflected in the topological properties of electron density.*

3.1 INTRODUCTION

The π-alkyne-complexes are one of the most important kind of transition-metal compounds. They are intermediate species in terminal alkyne to vinylidene rearrangements[1] and in homogeneous and heterogeneous catalytic reactions including hydrogenation,[2] hydrosilylation,[3] oligomerization,[4] polymerization,[5] metathesis,[6] condensation of terminal alkynes with several organic molecules (allyl alcohols,[7] α,β-unsaturated ketones,[8] alkenes,[9] dienes,[10] and alkynes[11]), cycloisomerization of 1,6-enynes,[12] and hydroamination.[13] In addition, they show applications in stoichiometric organic synthesis such as 2+2+2 and 2+2+1 cycloadditions,[14] quinone synthesis,[15] and complex condensations with carbenes.[16]

The broad range of applications of π-alkyne transition-metal complexes has also attracted the interest of theoretical chemists. Thus, several aspects of the coordination of alkynes to naked atoms,[17] surfaces,[18] and complexes[19] have been studied. Frenking and Fröhlich have recently reviewed these investigations.[20]

The chemical bonding in transition-metal alkyne complexes can be described in a similar way as for the transition-metal alkene complexes. A major difference between alkene and alkyne complexes is that the alkyne ligand has a second occupied π orbital orthogonal to the MC_2 plane ($\pi_\perp$) which, in some cases, engages in the transition-metal alkyne bonding. Then, the alkyne is a four-electron donor ligand by means of its $\pi_\parallel$ and $\pi_\perp$ orbitals.

The chemistry of four-electron donating alkynes has been centered at early-transition-metals, mainly molybdenum and tungsten.[21,22] Four-coordinated d^6 complexes of the types $ML(alkyne)_3$[23] and $ML_2(alkyne)_2$[24] have been also reported. In contrast, five-coordinate d^6 monoalkyne complexes with the general formula $ML_4(alkyne)$ are very scarce,[25] and MCpL(alkyne) are unknown.

Despite the high kinetic inertia of the $OsCpL_3$ compounds,[26] Esteruelas and coworkers have reported overwhelming evidences showing that the complex $Os(\eta^5\text{-}C_5H_5)Cl(P^iPr_3)_2$ is a labile starting material for the development of new cyclopentadienyl-osmium chemistry,[27] including $Os(\eta^5\text{-}C_5H_5)Cl(\eta^2\text{-alkyne})(P^iPr_3)$ complexes,[28] where the alkyne acts as a two-electron donor ligand. Now, they have discovered that these compounds can be converted into stable $[Os(\eta^5\text{-}C_5H_5)(\eta^2\text{-alkyne})(P^iPr_3)]^+$ species, containing a four-electron donating alkyne.

With regard to the complexes containing two-electron donor alkyne ligands, the donation from the $\pi_\perp$ orbital disturbs the molecular structure and reactivity[21,29] as well as spectroscopic properties[30] of the π-alkyne complex. Despite of the efforts made on the understanding of metal-alkyne bonding,[17-20] quantitative-theoretical studies on the

two-four-electron dichotomy of the alkyne ligands are still lacking. The discovery of complexes $Os(\eta^5\text{-}C_5H_5)Cl(\eta^2\text{-alkyne})(P^iPr_3)$ and $[Os(\eta^5\text{-}C_5H_5)(\eta^2\text{-alkyne})(P^iPr_3)]^+$ has prompted us to carry out theoretical calculations on the bonding scheme, geometries and bond energies, rotational barriers, and NMR properties in these unusual osmium-compounds.

In this chapter, we present the results of the theoretical study on the different bonding nature of the metal-alkyne interaction. The theoretical results are combined with the experimental work undertaken by the Prof. Esteruelas's group, which includes the synthesis and spectroscopic and X-ray characterization of $[Os(\eta^5\text{-}C_5H_5)(\eta^2\text{-alkyne})(P^iPr_3)]^+$, the X-ray characterization of $Os(\eta^5\text{-}C_5H_5)Cl(\eta^2\text{-alkyne})(P^iPr_3)$.

3.2 RESULTS AND DISCUSSION

3.2.1 Experimental Data on the Studied Chemical Systems

3.2.1.1 Synthesis, X-Ray and Spectroscopic Characterization of $Os(\eta^5\text{-}C_5H_5)Cl(\eta^2\text{-alkyne})(P^iPr_3)$ and $[Os(\eta^5\text{-}C_5H_5)(\eta^2\text{-alkyne})(P^iPr_3)]^+$

As a consequence of the large steric hindrance experienced by the triisopropylphosphine ligands of $Os(\eta^5\text{-}C_5H_5)Cl(P^iPr_3)_2$, in pentane, the splitting of a phosphorous-osmium bond is favored. Thus, the addition at room temperature of 1.2 equiv. of 1,1-diphenyl-2-propyn-1-ol and 2-methyl-3-butyn-2-ol to pentane solutions of this complex gives rise to the formation of the π-alkyne derivatives $Os(\eta^5\text{-}C_5H_5)Cl\{\eta^2\text{-}HC{\equiv}CC(OH)R_2\}(P^iPr_3)$ (R = Ph (**1a**), Me (**1b**)). In toluene solutions, at 85 ºC, complexes **1a** and **1b** evolve into the allenylidene $Os(\eta^5\text{-}C_5H_5)Cl(=C=C=CPh_2\}(P^iPr_3)$[27b] and alkenylvinylidene $Os(\eta^5\text{-}C_5H_5)Cl\{=C=CHC(CH_3)=CH_2\}(P^iPr_3)$,[28] respectively, with loss of a water molecule from the alkyne. Treatment at room temperature of dichloromethane solutions of **1a** and **1b** with $TlPF_6$ produces the extraction of the chloride ligand and the formation of $[Os(\eta^5\text{-}C_5H_5)\{\eta^2\text{-}HC{\equiv}CC(OH)R_2\}(P^iPr_3)]PF_6$ (R = Ph (**2a**), Me (**2b**)), which are isolated in high yield (Scheme 3.1). In contrast to **1a** and **1b**, **2a** and **2b** are stable in solution for long time. The dehydration of the alkyne, as well as their transformation into the corresponding allenylidene and alkenylvinylidene are not observed.

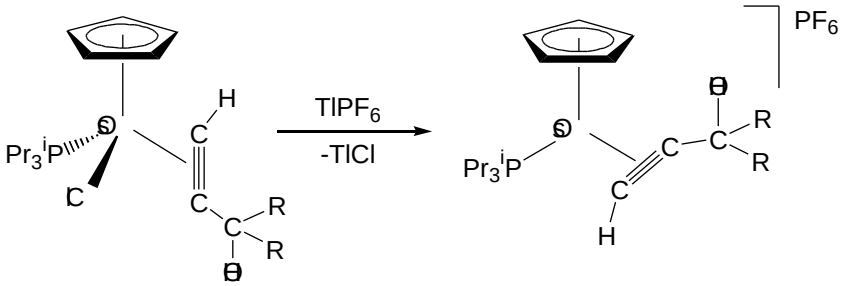

Scheme 3.1

Figure 3.1 shows the X-ray structures of **1a** and **2a**, whereas selected bond distances and angles for both compounds are listed in Table 3.1.

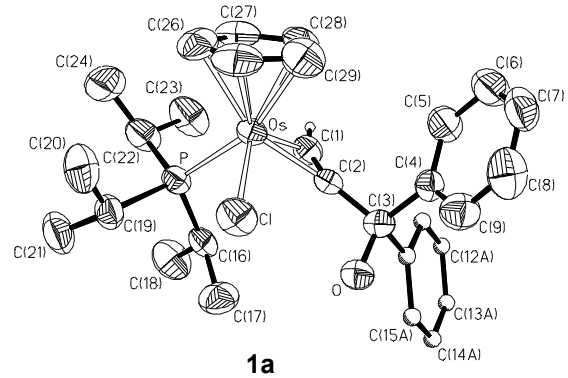

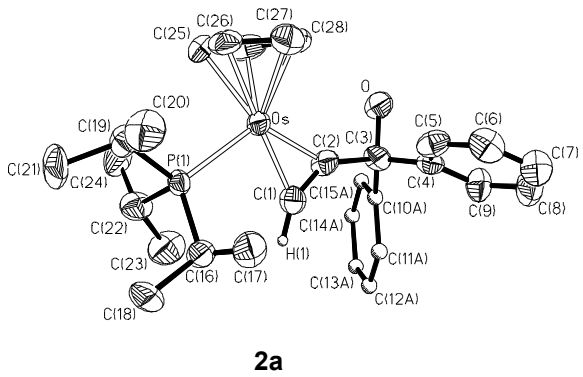

Figure 3.1. Molecular diagrams for the complex $Os(\eta^5\text{-}C_5H_5)Cl\{\eta^2\text{-}HC{\equiv}CC(OH)Ph_2\}(P^iPr_3)$ (**1a**) and for the cation of $[Os(\eta^5\text{-}C_5H_5)\{\eta^2\text{-}HC{\equiv}CC(OH)Ph_2\}(P^iPr_3)]PF_6$ (**2a**). Thermal ellipsoids are shown at 50% probability.

The geometry around the osmium atom of **1a** can be described as a three-legged piano-stool. The angles P-Os-Cl, P-Os-M(2) (M(2) is the midpoint of the carbon-carbon triple bond of the alkyne) and Cl-Os-M(2) are 86.85(6)º, 86.73(18)º, and 103.8(2)º, respectively.

Table 3.1. Selected Bond Distances (Å) and Angles (deg) for the Complexes Os(η^5-C_5H_5)Cl{η^2-HC≡CC(OH)Ph_2}(P^iPr_3) (**1a**) and [Os(η^5-C_5H_5){η^2-HC≡CC(OH)Ph_2}(P^iPr_3)]PF_6 (**2a**).

	1a	**2a**		**1a**	**2a**
Os-Cl	2.4445(16)		Os-C(27)	2.190(7)	2.180(11)
Os-P	2.3444(17)	2.410(2)	Os-C(28)	2.203(7)	2.205(9)
Os-C(1)	2.142(7)	1.992(9)	Os-C(29)	2.246(7)	2.205(9)
Os-C(2)	2.163(6)	1.981(8)	C(1)-C(2)	1.222(8)	1.26(2)
Os-C(25)	2.237(6)	2.222(7)	C(2)-C(3)	1.499(9)	1.513(11)
Os-C(26)	2.246(7)	2.220(9)			
Cl-Os-P	86.85(6)		Os-C(1)-C(2)	74.4(4)	71.1(6)
Cl-Os-M(1)[a]	115.5(3)		Os-C(1)-H(1)	125(5)	141(4)
Cl-Os-M(2)[a]	103.8(2)		Os-C(2)-C(1)	72.6(5)	72.0(5)
P-Os-M(1)	129.6(2)	119.2(4)	Os-C(2)-C(3)	137.8(5)	147.6(7)
P-Os-M(2)	86.73(18)	99.2(4)	H(1)-C(1)-C(2)	154(5)	145(4)
M(1)-Os-M(2)	121.0(3)	141.7(4)	C(1)-C(2)-C(3)	148.8(7)	140.3(9)

[a] M(1) and M(2) are the midpoints of the C(25)-C(29) Cp and C(1)-C(2) acetylenic ligands.

The carbon-carbon triple bond (C(1)-C(2)) forms an angle of 28º with the Os-Cl bond. The torsion angle Cl-Os-C(1)-C(2) is 156.3º, whereas the torsion angle P-Os-C(1)-C(2) is 112º. As expected, the coordination of the alkyne to the metal has a slight effect on the acetylenic bond length. Thus, the C(1)-C(2) distance (1.222(8) Å) is about 0.04 Å longer than the average value in free alkynes (1.18 Å).[31] The Os-C(1) (2.142(7) Å) and Os-C(2) (2.163(6) Å) bond lengths are statistically identical. In addition, it should be mentioned that the substituted carbon atom of the alkyne (C(2)) is away from the bulky triisopropylphosphine ligand. Although two isomers of **1a** could be formed in the solid state, this indicates that only one of them is obtained, that with less steric hindrance.

The geometry around the osmium atom of **2a** can be rationalized as a two-legged piano stool with the acetylenic C(1)-C(2) bond and the Os-P axis in the same plane. The P-Os-C(1)-C(2) torsion angle is 183.7º. Interestingly, although the C(1)-C(2)

bond lengths in **2a** (1.26(2) Å) and **1a** are very similar, there are substantial differences between the respective Os-carbon distances of both compounds. The Os-C(1) distance in **2a** (1.992(9)Å) is about 0.15 Å shorter than the related parameter in **1a**, whereas the Os-C(2) bond length in **2a** (1.981(8) Å) is about 0.18 Å shorter than that in **1a**. As in **1a**, the substituted C(2) carbon atom of **2a** is away from the phosphine ligand.

There are also substantial differences between the ^{1}H, $^{13}C\{^{1}H\}$ and $^{31}P\{^{1}H\}$ NMR spectra for complexes of types **1** and **2**. In the ^{1}H NMR spectra of **1a** and **1b** the HC≡ resonances of the alkynes appear at 4.3 and 3.73 ppm, respectively, as doublets with H-P coupling constants of about 9 Hz. The same HC≡ resonances for complexes **2a** and **2b** appear also as doublets but at lower field (about 9.3 ppm) and with H-P coupling constants (26.4 Hz for both compounds) much higher than those found in **1a** and **1b**. A similar relationship is observed in the $^{13}C\{^{1}H\}$ NMR spectra. In the $^{13}C\{^{1}H\}$ NMR spectra of **1a** and **1b**, the resonances corresponding to the acetylenic carbon atoms appear at 82.2 and 69.1 (≡CR), and at 57.5[32] and 49.6 (HC≡), while in the spectra of **2a** and **2b** they are observed at 179.0 and 182.8 (≡CR), and at 146.0 and 143.3 (HC≡) ppm, i.e. shifted about 100 ppm towards low field. The $^{31}P\{^{1}H\}$ NMR spectra also indicate that the electronic properties of osmium atoms in compounds of types **1** and **2** are different. While the chemical shifts of the singlets of **1a** and **1b** are 10.0 and 9.5 ppm, respectively, those of **2a** and **2b** are 38.0 and 36.3 ppm. These differences indicate that the alkyne ligand of **1a** and **1b** acts as a two-electron donor ligand, while in **2a** and **2b** it acts as a four-electron donor ligand.[30]

3.2.2 Computational Studies on the Alkyne Complexes

The differences in the alkyne-osmium bonding in compounds **1** and **2** has been studied by means of DFT calculations (B3LYP functional), in conjunction with Bader's Atoms in Molecules (AIM) theory. The study has been performed using $Os(\eta^5\text{-}C_5H_5)Cl(\eta^2\text{-}HC{\equiv}CH)(PH_3)$ (**A**) and $[Os(\eta^5\text{-}C_5H_5)(\eta^2\text{-}HC{\equiv}CH)(PH_3)]^+$ (**B**) as model systems of complexes of types **1** and **2**, respectively. Additionally, we have also considered $Os(\eta^5\text{-}C_5H_5)Cl(\eta^2\text{-}HC{\equiv}CCH_3)(PH_3)$ ($\mathbf{A^{CH3}}$) and $[Os(\eta^5\text{-}C_5H_5)(\eta^2\text{-}HC{\equiv}CCH_3)(PH_3)]^+$ ($\mathbf{B^{CH3}}$) in order to model the substituted alkynes.

3.2.2.1 Bonding Scheme

The way the alkyne ligand binds the metal center in complexes **A** and **B** can be analyzed first by using a fragment MO analysis.[33] In the former, the alkyne interacts with a 16-electron metal fragment of $d^6\text{-}[Os(\eta^5\text{-}C_5H_5)LL']$ type. Schilling et al. have shown that in such complexes, only the $\pi_{//}$ orbital of the alkyne interacts with a vacant

d orbital on the metal center, [34] this 2-electron-donor behavior leading to an 18-electron alkyne complex. A backdonation interaction, involving $\pi_{//}^*$, is also at work and was found to be responsible for the orientation of the alkyne with respect to the metal fragment. Complex **B** can be described as a 14-electron fragment of d^6-$[Os(\eta^5\text{-}C_5H_5)L]^+$ type interacting with an alkyne ligand in a geometry where the P, Os, C1 and C2 atoms are coplanar. There are now two vacant d orbitals on the metal fragment, one symmetrical and one antisymmetrical with respect to the molecular symmetry plane. The symmetry properties of these two empty d orbitals match that of the occupied $\pi_{//}$ and π orbitals (Figure 3.2a, b) so that the alkyne acts as a 4-electron-donor ligand, leading to an 18-electron complex. Note that a further stabilization results from the back-donation interaction which involves the $\pi_{//}^*$ orbital (Figure 3.2c). Similar orbital interaction schemes have been derived by Hoffmann and co-workers for d^4 molybdenum systems [35] and, more recently, by Decker and Klobukowski for the $M(CO)_3(C_2H_2)$ complexes (M = Fe, Ru).[19j] In each case, the participation of both the $\pi_{//}$ and π orbitals in donating electrons to the metal allows the complex to reach the 18-electron count. This qualitative analysis, derived from the DFT computed molecular orbitals, is further supported by NBO (Natural Bonding Orbitals) population analysis carried out on complexes **A** and **B**. The population of the alkyne π NBO orbital is significantly lower in B (1.679 *e*) than in **A** (1.982 *e*), showing that π is involved in the alkyne-metal bonding in **B** but not in **A**. Note that in both complexes, the participation of π^* is almost negligible, the NBO population being equal to 0.017 *e* and 0.042 *e* in **A** and **B,** respectively.

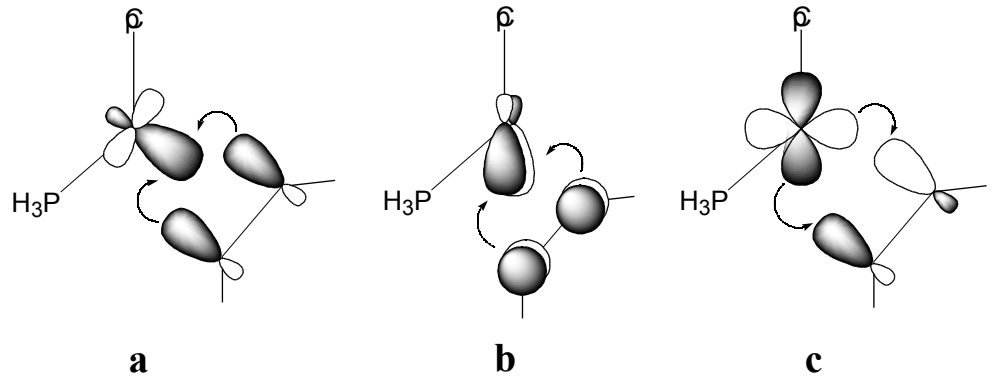

Figure 3.2. Schematic representation of the donative (a and b) and backdonative (c) interactions for metal-alkyne bonding in complex $[Os(\eta^5\text{-}C_5H_5)(\eta^2\text{-}HC{\equiv}CH)(PH_3)]^+$ (**B**).

This qualitative analysis shows that the alkyne ligand acts as a two- and a four-electron donor in complexes **A** and **B**, respectively. Therefore, these two parent complexes provide the opportunity to study how the geometrical, electronic and

energetic properties of an alkyne complex depend on the donor behavior of that ligand.

3.2.2.2 Geometries and Bond Energies

The computed optimized geometries of complexes $Os(\eta^5\text{-}C_5H_5)Cl(\eta^2\text{-}HC{\equiv}CR)(PH_3)$ (R = H (**A**), CH_3 (**A**^{CH3})) and $[Os(\eta^5\text{-}C_5H_5)(\eta^2\text{-}HC{\equiv}CR)(PH_3)]^+$ (R = H (**B**), CH_3 (**B**^{CH3})) are presented in Figure 3.3. In **A**, the C≡C acetylene bond forms an angle of about 25º with the Os-Cl bond. The computed torsion angle between P-Os-C1-C2 atoms is 106.0º for complex **A**, while for **B** is 179.9º, indicating that acetylenic carbons, osmium, and phosphorus atoms are almost coplanar in complex **B**. These results agree with the alkyne conformations of the X-ray-determined structures. The differences in conformational preferences of the two complexes will be commented upon later. In the case of substituted alkynes (R = CH_3), two different isomers have been considered for each complex (**A**^{CH3} and **B**^{CH3}), depending on which acetylenic carbon is substituted. Thus, the methyl substituent can lie in the phosphine ligand side (*endo*) or in the opposite side (*exo*). The *endo* isomers (**An**^{CH3} and **Bn**^{CH3}) are 0.8 and 2.8 kcal.mol^{-1} higher in energy than their respective *exo* forms (**Ax**^{CH3} and **Bx**^{CH3}) for complexes **A**^{CH3} and **B**^{CH3}, respectively. This result agrees with the experimental data, since the X-ray structures of complexes **1a** and **2a** correspond to *exo* forms. In the following, the discussion on substituted acetylenes will therefore concentrate on the *exo* isomers.

In Table 3.2 are summarized the most relevant theoretical parameters, together with those reported for experimental complexes **1a** and **2a**. Optimized geometries were found to be close to experimental ones for both alkyne complexes. The most interesting aspect of our computed geometrical parameters is that we succeeded in reproducing structural changes between complexes **1a** and **2a**. As we go from **A** to **B** the Os-C1 and Os-C2 distances decrease by 0.162 and 0.159 Å, respectively, and C1-C2 increases by only 0.034 Å. These results reflect the two-electron *vs* four-electron behavior of the alkyne ligand in complexes **A** and **B**, respectively. It compares nicely with the geometry changes previously reported between $Os(CO)_4(C_2H_2)$ to $Os(CO)_3(C_2H_2)$complexes[19j] at similar level of calculation. In the former (two-electron donor acetylene ligand), the Os-C(acetylene) bond distance is longer than in the latter (four-electron donor acetylene ligand) by 0.189 Å (2.220 *vs* 2.031 Å), while the C-C distance is shorter by 0.053 Å (1.276 *vs* 1.329 Å). The bond length values for tetra- and tricarbonyl species are actually close to our computed values for complexes **A** and **B**, respectively (Table 3.2).

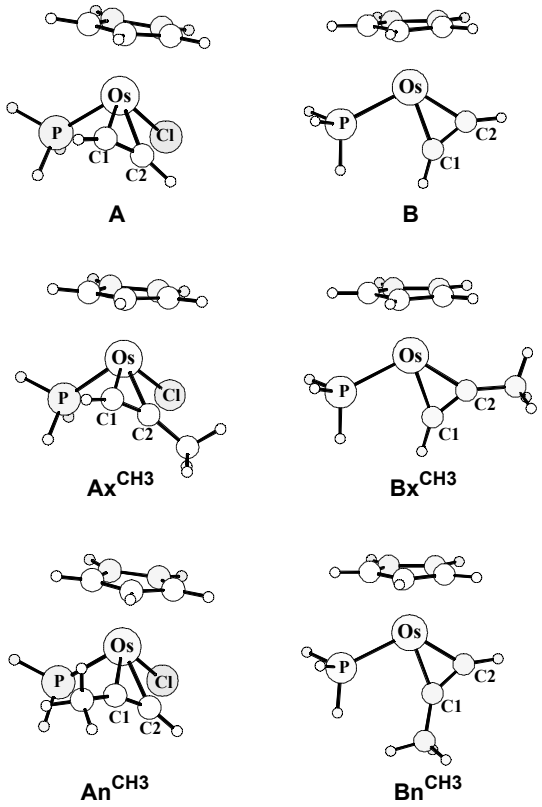

Figure 3.3. Optimized B3LYP geometries of the alkyne complexes $Os(\eta^5\text{-}C_5H_5)Cl(\eta^2\text{-}HC{\equiv}CR)(PH_3)$ (R = H (**A**), CH_3 (**A**$^{\mathbf{CH3}}$)), and $[Os(\eta^5\text{-}C_5H_5)(\eta^2\text{-}HC{\equiv}CR)(PH_3)]^+$ (R = H (**B**), CH_3 (**B**$^{\mathbf{CH3}}$)).

Table 3.2. Experimental and Calculated Geometric Parameters,[a] and Calculated Bond Dissociation Energies.[b]

Parameters	**1a**	**A**	**Ax^{CH3}**	**2a**	**B**	**Bx^{CH3}**
Os-C1	2.142(7)	2.176	2.168	1.992	2.014	2.000
Os-C2	2.163(6)	2.150	2.182	1.981(8)	1.991	2.004
C1-C2	1.222(8)	1.265	1.266	1.26(2)	1.299	1.305
C1-C2-R	148.8(7)	152.6	152.4	140.3(9)	146.2	145.9
C2-C1-H	154(5)	152.6	152.0	145(4)	146.0	145.5
P-Os-C1-C2	112	106.0	105.7	183.7	179.9	180.1
De		23.0	21.1		69.6	71.1

[a] Bond legths in Å and bond angles in degrees. [b] Alkyne-osmium bond dissociation energies (De) in kcal.mol^{-1}.

The coordination of alkyne ligand induces not only a lengthening of the C1-C2 distance (1.18 Å in free alkyne) [31] but also a bending of the substituents away from the metal. The calculated bond angles of C2-C1-H moieties are 153º for complex **A** and 146º for **B**, in excellent agreement with the experimental values for **1a** (154(5)º) and **2a** (145(4)º). Finally, note that no significant differences in geometrical parameters were observed upon introduction of methyl substituent onto the acetylene ligand (**Ax**^{CH3} and **Bx**^{CH3}).

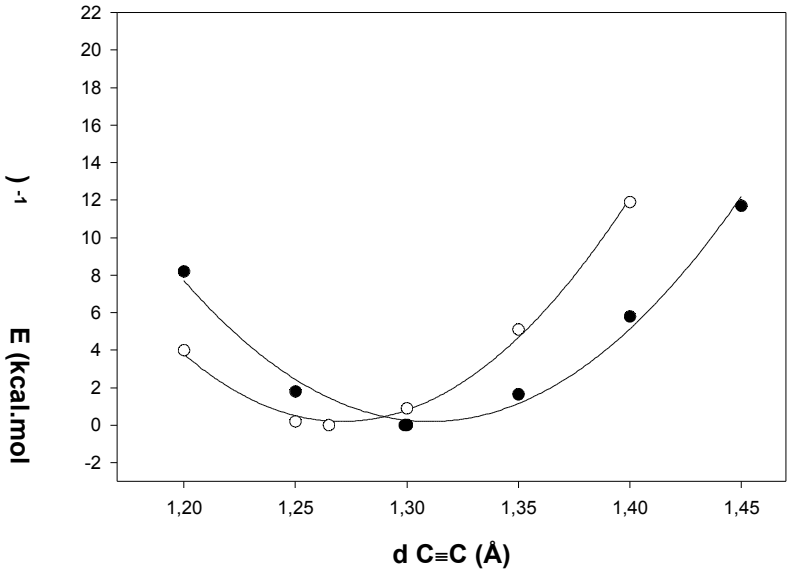

Figure 3.4. Potential energy surface for the C≡C distance in Os(η^5-C_5H_5)Cl(η^2-HC≡CH)(PH_3) (_, **A**) and [Os(η^5-C_5H_5)(η^2-HC≡CH)(PH_3)]$^+$ (· , **B**) model systems.

It may be stated from the geometrical analysis that the behavior of the alkyne ligand as a donor of two or four electrons (2e or 4e) is reflected in both metal-carbon and carbon-carbon bond distances. Thus, when the alkyne acts as a 4e donor ligand there is a contraction of the M-C bond, and the C-C bond is slightly elongated. The average experimental values of C-C distances in the coordinate terminal alkynes are 1.271 and 1.309 Å for 2e and 4e donor ligands, respectively.[36] It is interesting to notice that the X-ray-determined C-C distances for our osmium systems are shorter than these average values. Furthermore, the C-C distance of complex **2a**, in which the alkyne acts as a 4e donor ligand, is in the range of the average value for 2e donor ligands. The reliability of C-C alkyne distance as an indicator of 2e or 4e donor ligand

was studied by computing the monodimensional Potential Energy Surface (PES) for the C-C coordinate in **A** and **B** complexes. The PES was built by varying the C-C distance from their equilibrium values, and optimizing the rest of the complex at each point. The C-C distances that can be reached within an energy excess of 3 kcal.mol^{-1} with respect to the minimum energy structure range from 1.209 to 1.333 Å for complex **A**, and from 1.243 to 1.378 Å for complex **B**. This is what we could call the flexibility range of the C≡C bond. The calculated PES is flat (Figure 3.4), and therefore a wide range of C-C distances can be reached with low energy cost. Thus, the equilibrium distance of **A** (1.265 Å) is within the range of flexibility of **B**, and at the same time, the equilibrium distance of **B** (1.299 Å) is within the range of flexibility of complex **A**. The calculations show clearly that the C≡C bond lengths are not a reliable indicator of the metal-alkyne coordination mode.

Table 3.2 gives also the theoretically predicted alkyne bond dissociation energies (De) of **A**, **B**, $\mathbf{Ax}^{\mathbf{CH3}}$ and $\mathbf{Bx}^{\mathbf{CH3}}$. The bond energies are calculated as the energy difference between the complex on the one hand, and the ligand and the metal fragment at their respective optimized geometries, on the other hand. The predicted De for **B** (69.6 kcal.mol^{-1}) is substantially higher than De for the parent complex **A** (23.0 kcal.mol^{-1}). The stronger De of acetylene in **B** than in **A** can be attributed to the bond contribution of the acetylene second π system (π) in the former. Similar bond energies were calculated for methyl-substituted acetylene: 21.1 and 71.1 kcal.mol^{-1} for $\mathbf{Ax}^{\mathbf{CH3}}$ and $\mathbf{Bx}^{\mathbf{CH3}}$, respectively. It should be mentioned that the computed value of De for complex **B** (69.6 kcal.mol^{-1}) is higher than those usually reported in previous theoretical studies on alkyne-metal bonding.[20] However, in a recent contribution similar values were calculated at CCSD(T) level for $Ni(C_2H_2)_2$ and $Ni(PH_3)_2(C_2H_2)_2$ complexes, 66.9 and 62.6 kcal.mol^{-1}, respectively.[19i] For both nickel complexes, it was suggested a bonding contribution of acetylene's second π system. A bond-length/ bond-strength correlation between the two acetylene complexes **A** and **B** is observed. The Os-C1 and Os-C2 bond distances of **B** are shorter than those of **A** and the metal-acetylene De of **B** is much higher than that of **A** (Table 3.2). Thus, a shortening of osmium-alkyne distance increases the metal-ligand interaction. Therefore, we can state that the 4e alkyne ligands are more strongly bonded to the metal than their respective 2e alkyne ligands, due to the bonding contribution of the second π system of the alkyne.

3.2.2.3 Rotational Barriers

The transition states for the acetylene rotation were located for both **A** and **B** complexes and characterized by calculation of the Hessian matrix.

In complex **A**, the transition state (**Arot**, Figure 3.5) was found to be located 11.4 kcal/mol above the minimum. In this structure, the dihedral angle between C≡C and Os-Cl bonds is equal to 50.7°. The values of the Os-Cacetylene distances are 2.300 and 2.198 Å and the C≡C distance is 1.245 Å. Comparison with the geometry of the minimum energy structure **A** (Table 3.2) shows that the rotation induces a lengthening of the M-C distances accompanied by a shortening of the C-C distance. These changes between **A** and **Arot** can be rationalized by the orbital arguments developed by Hoffmann et al.:[34] the lengthening of the Os-C distances upon rotation of the acetylene ligand results from the increase of the Os-π repulsive interaction, while the shortening of the C≡C bond is related to the decrease of the back donation to the $\pi_{//}^{*}$ orbital. **Arot** remains however an 18-electron species in which the acetylene acts as a two-electron donor ligand.

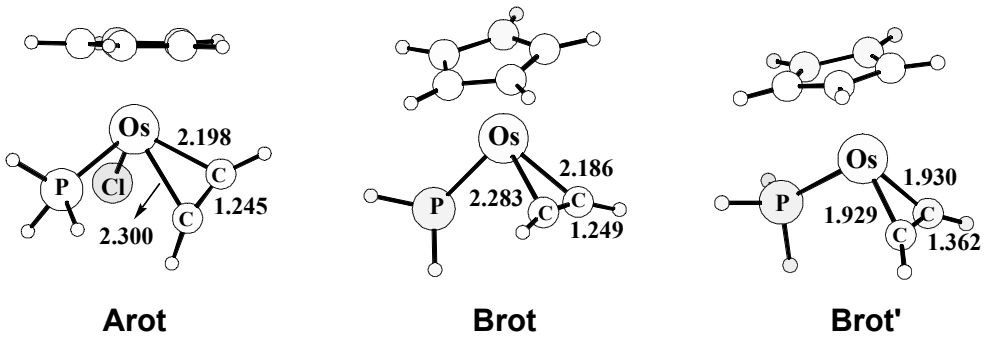

Figure 3.5. Optimized B3LYP geometries of **Arot**, **Brot** and **Brot'** structures. Bond distances are given in Å.

The situation is more complicated for complex **B** since *two* saddle points were characterized for the rotational process of acetylene. In the first one (**Brot**, Figure 3.5), the optimized geometrical parameters are rather similar to those given just above for **Arot**, with Os-Cacetylene distances of 2.186 and 2.283 Å and C-C distance of 1.249 Å. Despite this geometrical similarity, the computed energy barrier is much higher since **Brot** is located 32.7 kcal/mol above the minimum energy structure **B**. This remarkably high value for the rotational barrier can be explained by using the symmetry properties of the fragment molecular orbitals displayed in Figure 3.2. We have previously mentioned that in the equilibrium structure **B** the filled π orbitals, $\pi_{//}$ and π, are respectively symmetric (a') and antisymmetric (a'') with respect to molecular symmetry plane, so that each of them can interact with one of the two low lying d orbitals of the metal fragment (π with a'' and $\pi_{//}$ with 1a', Figure 3.2). Therefore, in the equilibrium structure, the acetylene ligand plays the role of a four-electron donor. In the transition state structure, the acetylene is rotated by 90°.

Assuming an idealized C*s* symmetry, both $\pi_{//}$ and π become symmetric, so that the overlap between π and the a'' metal fragment orbital vanishes. The electron donation from π is thus lost and the only significant interaction which remains is that between $\pi_{//}$ and the 1a' orbital. The high value computed for the rotational barrier can thus be traced to the change of the electron donor character of the acetylene ligand on going from **B** (four-electron, 18-electron species) to **Brot** (two-electron, 16-electron species). This qualitative analysis, consistent with the evolution of the geometrical parameters, is further supported by the NBO analysis. The population of the alkyne π NBO is significantly smaller for complex **B** (1.679 *e*) than for the transition state **Brot** (1.984 *e*) in which this orbital is almost full. These results show that π is involved in alkyne-metal bonding in the stable complex, **B**, but not in **Brot** structure.

As mentioned above, a second transition state was found for the acetylene rotation (**Brot'**, Figure 3.5). Its geometry strongly differs from that of **Brot**: the Os-Cacetylene distances (1.930 and 1.929 Å) are shortened about 0.3 Å, and the C-C distance (1.362 Å) lengthened by 0.113 Å. Note that this later value is greater than that for free ethylene (1.336 Å). These geometrical features clearly indicate the nature of the metal-acetylene bonding in **Brot'** cannot be described in terms of donor-acceptor interactions following the Dewar-Chatt-Ducanson model.[37] It is better to consider **Brot'** as a metallacycle with two Os-C single bonds and a double bond between the carbon atoms, instead of an alkyne complex. Last but not least, **Brot'** was found to be lower in energy than **Brot** by 8.4 kcal/mol. Consequently, the lowest energy path for the rotation of the alkyne ligand in complex **B** involves the metallacycle **Brot'** as transition state structure. The activation energy remains high (24.3 kcal/mol) compared to that for complex **A**, because **Brot'** is still a 16-electron species.

Brot and **Brot'** can be seen as two structures along with the reaction path for the perpendicular approach of an acetylene molecule toward the $CpOs(PH_3)^+$ metal fragment. Since both have been characterized as saddle points for the acetylene rotational process, it means that an energy barrier should be encountered on going from **Brot** to **Brot'** by decreasing the Os-acetylene distance. The origin of this barrier, which makes possible to optimize separately an acetylene (**Brot**) and a metallacyclopropene (**Brot'**) complex, lies in *a change of the ground electronic configuration*, schematically depicted on Figure 3.6, which in turn reflects the different chemical nature of two complexes. Let us assume an idealized C*s* symmetry to analyze the origin of this orbital crossing. In **Brot** ("long" Os-C distance), the HOMO (a') is the antibonding combination of the filled π ligand orbital with a filled metal fragment orbital and the LUMO (a'') a bonding combination of $\pi_{//}^*$ with the filled a'' orbital on the metal fragment (Figure 3.6, right-hand-side). Going from **Brot** to **Brot'** entails a shortening of Os-C distances and a lengthening of the C-C distance. The HOMO (a'), Os-C antibonding and C-C bonding is thus destabilized, while the

LUMO (a''), Os-C bonding and C-C antibonding, is stabilized. A crossing occurs between these occupied and vacant molecular orbitals, which results in an energy barrier between these two structures (reaction path "forbidden by symmetry"). Note that in turn the change from a'^2 to a''^2 ground state configuration is consistent with a shortening of the M-Cacetylene distances (antibonding M-C -> bonding M-C) and a lengthening of the C-C distance (bonding C-C -> antibonding C-C) on going from **Brot** to **Brot'**.

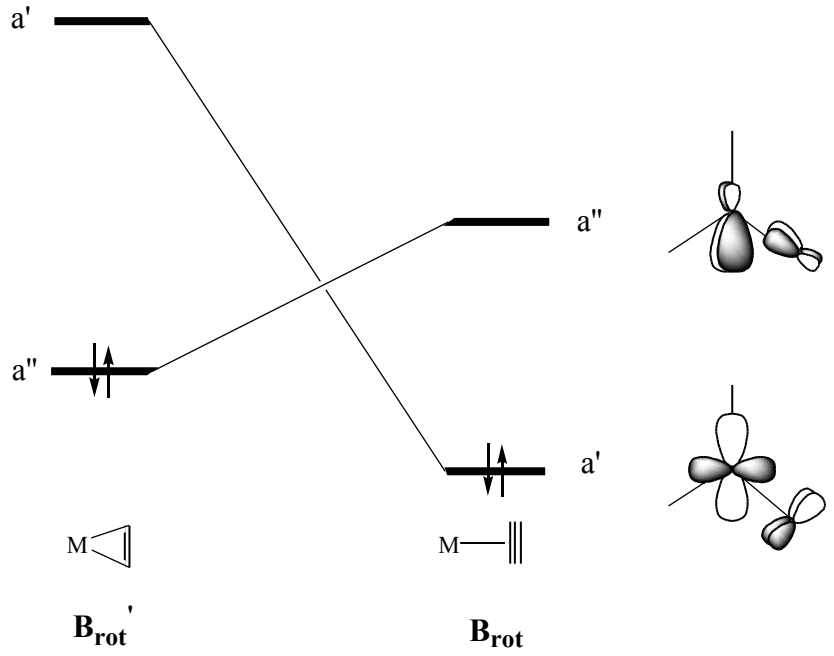

Figure 3.6. Schematic drawing of the frontier molecular orbital crossing found on going from **Brot** to **Brot'**.

3.2.2.4 NMR Properties

We have carried out theoretical studies on the NMR properties of model complexes **A**, $\mathbf{Ax}^{\mathbf{CH3}}$, **B**, and $\mathbf{Bx}^{\mathbf{CH3}}$ by using the Gauge-Including Atomic Orbitals (GIAO) method.[38] The ^{13}C and ^{1}H chemical shifts were calculated with respect to tetramethylsilane. Recently, GIAO method has been successfully used in the study of NMR properties of acetylenes coordinated to a transition metal by Walther and co-workers.[19i]

Table 3.3 collects the experimental and calculated chemical shifts, as well as the NPA charges on acetylenic carbons. The calculated chemical shifts are in the range

found experimentally and reproduce the trend observed on going from **1** to **2**. Calculated $\delta(^{13}C)$ for **B** (145.3 and 157.3 ppm) are significantly higher than those for **A** (68.7 and 104.2 ppm). The same trend is observed for the calculated $\delta(^{1}H)$, 4.4 ppm for **A** and 8.9 ppm for **B**. When a methyl group replaces one of the acetylenic hydrogens (**Ax**^{CH3} and **Bx**^{CH3}), $\delta(^{13}C)$ and $\delta(^{1}H)$ still better fit the experimental values. The NMR properties are very sensitive to electronic variations and, therefore, the use of a simple alkyne model could be one source of error on computed chemical shifts, especially for substituted acetylenic carbons. However, we have succeeded in reproducing qualitatively the differences between a two-electron and a four-electron donor alkyne complex.

Table 3.3. NMR ^{13}C and ^{1}H Chemical Shifts (ppm) Relative to TMS, and NPA Charges.[a]

Parameters	**1a**	**1b**	**A**	**Ax**^{CH3}	**2a**	**2b**	**B**	**Bx**^{CH3}
$\delta(^{13}C)$ C1	57.5	49.6	68.7	57.7	146.0	143.3	145.3	144.8
$\delta(^{13}C)$ C2	82.2	69.1	104.2	102.6	179.0	182.8	157.3	175.0
$\delta(^{1}H)$ H[b]	4.32	3.72	4.4	3.7	9.43	9.9	8.9	8.8
q (C1)[c]			-0.08	-0.10			-0.04	-0.05
q (C2)[c]			0.04	0.00			0.05	0.10
q (H)			0.25	0.25			0.28	0.28

[a] Charges in atomic units. [b] Chemical shifts for terminal acetylenic hydrogens. [c] The charges of substituents have been added to the charge of acetylenic carbons.

Additionally we have computed the ^{13}C and ^{1}H chemical shifts of the saddle points for acetylene rotation (**Arot**, **Brot** and **Brot'**). The average values of calculated $\delta(^{13}C)$ for acetylenic carbons of **Arot** species (77.8 ppm) and **Brot** species (69.7 ppm) are similar, and closer related to complex **A** than to complex **B** (Table 3.3). On the other hand, the average value for **Brot'** (249.3 ppm) is much higher than those computed for **A** and **B** complexes. These results indicate that the bonding scheme in **Arot** and **Brot** structures resemble that in complex **A**, in which the acetylene ligand acts as a two-electron donor, while in **Brot'** differs from those in **A** and **B**. Thus, computed NMR properties further support the arguments stated in previous section about the bonding nature of rotational structures.

The ^{13}C chemical shift values are roughly indicative of the electronic density around that atom. The atom most shifted is the least shielded one and, consequently, the poorest in electrons. Thus, one could expect a correlation between the atomic charges and the chemical shift of the acetylenic coordinated carbons, in such a way that the least charged carbon is the most shifted. The calculated NPA charges of

acetylenic carbons are consistent with this argument for a given complex (Table 3.3). Also, NPA charges show that acetylenic carbons are less charged for the 4e donor acetylene complex **B** (-0.04 and 0.05 e) than for 2e donor **A** (-0.08 and 0.04 e), the **B** complex exhibiting the most shifted carbons. Despite variations in atomic carbon charges, the small differences (≤ 0.04 e) do not seem to justify the considerable variation in chemical shifts observed for the two bonding situations. Note, however, that the two complexes carry a different total net charges, which could mask the differences in atomic charges, hindering a direct comparison between them. Apart from atomic charges, chemical shifts may be also related to the occupancies of acetylenic molecular orbitals. From the NBO analysis we found that in complex **B** the π orbital is significantly depopulated (1.679 e), while for complex **A** is full (1.982 e). Thus, in the line of previous arguments, when alkyne the ligand acts as a four-electron donor there is a decrease of electron population on acetylenic carbons, which become more deshielded and, consequently, appear at low-field resonance, i.e., highly shifted.

3.2.2.5 Bader Analysis

The metal-alkyne bonding has been also investigated by means of Bader analysis of the electron density. Bader's Atoms in Molecules (AIM) theory provides a set of practical tools for the study of bonding properties.[39] The Os-C and C≡C interactions were characterized by critical points (cp's) in the electronic charge density ($\rho(r)$), which are points in the space where $\rho(r)$ vanishes. According to Bader's theory, the localization of a bond critical point (bcp) between two atoms proves the existence of an interaction between them, while the ring critical point (rcp) is characteristic of atomic rings. The values of $\rho(r)$, Laplacian ($^2\rho(r)$) and ellipticity (ε) at the critical points were used to gauge the variation in charge density and bonding properties for the complexes under study.

In Table 3.4 are summarized the results of topological analysis of electron density, for acetylene and propyne complexes, as well as for the saddle points of the rotational process. In a first inspection of data collected in Table 3.4, some general trends can be observed. The values of the Laplacian at the bcp ($^2\rho_{CP}$) are relatively low and positive for all the Os-Calkyne bonds, except for **Brot'** structure. Thus, according to AIM theory, the relatively low and positive value of the Laplacian at the bcp indicates a closed-shell interaction. On the other hand, for C≡C bonds the values of $^2\rho_{cp}$ (large and negative) are indicative of shared interactions, characterized by a large accumulation of charge between the nuclei.

Table 3.4. Topological Properties of the Electron Density at the Bond and Ring Critical Points.[a]

		A	Ax^{CH3}	Arot	B	Bx^{CH3}	Brot	Brot'
Os-C1	ρ_{cp}	0.097	0.099	0.075	0.138	0.142	0.075	0.165
	$^2\rho_{cp}$	0.158	0.143	0.161	0.185	0.177	0.170	0.272
Os-C2	ρ_{cp}	0.101	0.096	0.090	0.143	0.140	0.091	0.164
	$^2\rho_{cp}$	0.180	0.174	0.153	0.212	0.205	0.155	0.276
C1-Os-C2[b]	ρ_{cp}	0.090	0.089	0.074	0.124	0.124	0.075	0.144
	$^2\rho_{cp}$	0.360	0.348	0.276	0.472	0.469	0.248	0.505
C1-C2	ρ_{cp}	0.377	0.376	0.388	0.363	0.359	0.373	0.328
	$^2\rho_{cp}$	-1.041	-1.095	-1.156	-1.041	-1.021	-1.096	-0.856
	ε	0.189	0.210	0.183	0.024	0.030	0.145	0.075

[a] Electron charge density, ρ_{cp}, Laplacian, $^2\rho_{cp}$, and ellipticity, ε, in atomic units. [b] Ring critical point

The two kinds of acetylene complexes, **A** and **B**, present differences in the topological properties of electron density for the osmium-acetylene interactions. Larger values of $\rho(r)$ at the bcp (ρ_{CP}) for Os-C bonds are observed in the four-donor acetylene complex **B** (Table 3.4). The value of ρ_{CP} is related with the bond order, and can be considered a measure of the bond strength, in such a way that the larger ρ_{CP} is the stronger is the bond. Thus, these results are consistent with our previous findings, which indicated an increase in the strength of the metal-acetylene bond when the π orbital participated in the bonding. The calculated values of ρ_{CP} for Os-C bonds increase by 0.04 e, from 0.097 and 0.101 e in **A** to 0.138 and 0.143 e in **B**. These values nicely compare with those reported by Decker and Klobukowski for $Ru(CO)_4(C_2H_2)$ and $Ru(CO)_3(C_2H_2)$ complexes,[19j] in which it was found that acetylene ligand acts as two-electron and four-electron donor, respectively. In the Ru complexes the ρ_{CP} increase also by 0.04 e, from 0.075 e in the tetracarbonyl complex to 0.110 e in the tricarbonyl one. Moreover, ring critical points were found between the Os and the acetylenic carbons, and a larger value of ρ_{CP} was observed in complex **B** for the metallacyclopropene-like ring. For C-C acetylene bonds the value of ρ_{CP} decreases on going from complex **A** to **B**, suggesting a weakening of acetylene bond. However, the decrease in the amount of ρ_{CP} is small, only 0.01 e (from 0.377 e in **A** to 0.363 e in **B**). This is not surprising, since we have shown in a previous section that the C≡C bond is relatively flexible: i.e., that a wide range of C-C distances can be reached with low energy cost. Neither the C-C bond lengths nor the values of $\rho(r)$ at the C-C bcp are reliable indicators of the metal alkyne coordination mode. In spite of this, significant differences were found in the values of ellipticity (ε) for the C-C bonds between the

two complexes (Table 3.4). The ellipticity provides a measure for the π character of the bond, thus, large values of ellipticity are indicative of high π bond character. The low value of ε at the C-C bcp in **B** (0.024 e) can be related with the participation of two π orbitals instead of one in the bonding, which will decrease the π character of the acetylene. We have focused our discussion on the topological analysis of acetylenic complexes; however, the same argumentation could be drawn for the methyl-substituted acetylenic complexes $\mathbf{Ax}^{\mathbf{CH3}}$ and $\mathbf{Bx}^{\mathbf{CH3}}$. In summary, the differences in coordination mode of alkyne complexes are reflected in the properties of the electron density topology, in both, the values of ρ_{CP} at the Os-C bonds and ε at the C-C bcp. Therefore, when the two π orbitals of alkyne participate in the bonding higher values of ρ_{CP} and lower values of ε are expected.

Additionally, we have performed the topological analysis of electron density for osmium-acetylene interaction in the saddle points for acetylene rotation (**Arot**, **Brot** and **Brot'**). The topological properties in **Arot** and **Brot** species are very similar for both ρ(r) and ε at the bcp's. The values of ρ_{CP} at the Os-C bonds and ε at the C-C bcp's better compare to the values found in the acetylene complex **A** than in **B**, further proving the two-electron coordination of acetylene in these rotational species. However, somewhat lower values of ρ_{CP} at the Os-C bonds were observed in **Arot** and **Brot**, indicating a weakening of the Os-acetylene bonding. The **Brot'** structure presents a significant increase in the values of ρ_{CP} at the Os-C bonds and a decrease at the C-C acetylenic bonds, reaching respectively, larger and lower values than those of complex **B**. In addition relatively large values of ($^2\rho_{CP}$) at the Os-C bonds were observed, suggesting a change in the nature of the metal-alkyne interaction for **Brot'** species, in agreement with previous findings.

3.3 CONCLUDING REMARKS

Treatment of the π-alkyne complexes $Os(\eta^5\text{-}C_5H_5)Cl\{\eta^2\text{-}HC{\equiv}CC(OH)R_2\}(P^iPr_3)$ (**1**) with $TlPF_6$ produces the extraction of the chloride ligand and the formation of $[Os(\eta^5\text{-}C_5H_5)\{\eta^2\text{-}HC{\equiv}CC(OH)R_2\}(P^iPr_3)]PF_6$ (**2**). The extraction of the chloride ligand from **1** generates an interaction between an empty d orbital of the osmium atom and the π orbital of the alkyne. As a result, the structural parameters and the spectroscopic properties of the alkyne undergo significant disturbances. The Os-alkyne distances are shortened, and in the $^{13}C\{^1H\}$ and ^1H NMR spectra, the chemical shifts of the acetylenic carbon and HC≡ resonances are shifted toward lower field. Theoretical calculations on the model compounds $Os(\eta^5\text{-}C_5H_5)Cl(\eta^2\text{-}HC{\equiv}CR)(PH_3)$ (**A**) and $[Os(\eta^5\text{-}C_5H_5)\{\eta^2\text{-}HC{\equiv}CR\}(PH_3)]^+$ (**B**) suggest that the disturbance in the chemical shifts is a consequence of the depopulation of the π orbital of the alkyne, on

going from **1** to **2** or from **A** to **B**. Both structural and spectroscopic changes are in accord with the rationale of an increased donation from the alkyne, as a consequence of the participation of the acetylenic second π orbital (π) in the bonding.

The theoretical calculations also predict that, in this type of systems, the interaction between the π orbital of the alkyne and an empty d orbital of the osmium gives rise to an increase of the dissociation energy of the alkyne, and an increase of the energy for the rotation of the alkyne around the osmium-alkyne axis. The enhancement in the rotational barrier is due to the loss of the π → M interaction, which makes rotation proceed via a formally unsaturated 16-electron path. The results of topological properties of the electron density of the system also reflect the π → M interaction, and are in full agreement with previous findings. As we go from **A** to **B**, we observe an increase of electron density at the bcp between the metal and the acetylenic carbon atoms, which is accompanied by a decrease of ε at the bcp between the two acetylenic carbons. These results are consistent with an increase in the amount of bonding between the alkyne ligand and the metal.

3.4 COMPUTATIONAL DETAILS

Calculations were performed with the GAUSSIAN 98 series of programs[40] within the framework of the Density Functional Theory (DFT)[41] using the B3LYP functional.[42] A quasirelativistic effective core potential operator was used to represent the 60 innermost electrons of the osmium atom.[43] The basis set for the metal atom was that associated with the pseudopotential,[43] with a standard double-ζ LANL2DZ contraction.[40] The 6-31G(d,p) basis set was used for the P, Cl and C atoms directly attached to the metal, whereas the 6-31G basis set was used for the hydrogen atoms.[44] In the case of propyne model complexes ($\mathbf{A}^{\mathbf{CH3}}$ and $\mathbf{B}^{\mathbf{CH3}}$) the C and H atoms of methyl substituent were described using a 6-31G basis set. [44] Geometry optimizations were carried out without any symmetry restrictions and all stationary points were optimized with analytical first derivatives. Saddle points were located by means of approximate Hessians and synchronous transit-guided quasi-Newtonian methods.[45] All saddle points were characterized by means of normal modes analysis, with one imaginary frequency corresponding to rotation of acetylene ligand. In the case of **Brot** and **Brot'**, additional calculations were performed in order to further confirm that both saddle points correspond to the acetylene rotational process. Displacements in atomic coordinates following the normal mode of the imaginary frequencies were made, and in both species, the subsequent optimization processes led to the reactant and product of the process.

Nuclear magnetic resonance (NMR) properties have been computed by using the Gauge-Independent Atomic Orbital (GIAO) method.[38] The bonding situation of the complexes has been analyzed with the help of the NBO partitioning scheme.[46] Furthermore, atomic charges have been calculated by means of Natural Population Analysis (NPA) method.[46] The topological properties of the electron density[39] were investigated using the XAIM 1.0 program.[47]

REFERENCES

1. (a) Silvestre, J.; Hoffman, R. *Helv. Chem. Acta* **1985**, *68*, 1461. (b) Bruce, M.I. *Chem. Rev.* **1991**, *91*, 197. (c) Lomprey, J. R.; Selegue, J. P. *J. Am. Chem. Soc*. **1992**, *114*, 5518. (d) Werner, H. *J. Organomet. Chem.* **1994**, *475*, 45. (e) Wakatsuki, Y.; Koga, N.; Yamazaki, H.; Morokuma, K. *J. Am. Chem. Soc*. **1994**, *116*, 8105. (f) de los Ríos, I.; Jiménez-Tenorio, M.; Puerta, M. C.; Valerga, P. *J. Chem. Soc.; Chem. Commun*. **1995**, 1757. (g) Wakatsuki, Y.; Koga, N.; Werner, H.; Morokuma, K. *J. Am. Chem. Soc.* **1997**, *119*, 360. (h) de los Ríos, I.; Jiménez-Tenorio, M.; Puerta, M. C.; Valerga, P. *J. Am. Chem. Soc*. **1997**, *119*, 6529. (i) Bruneau, C.; Dixneuf, P. H. *Acc. Chem. Res.* **1999**, *32*, 311. (j) Bustelo, E.; Jiménez-Tenorio, M.; Puerta, M. C.; Valerga, P. *Organometallics* **1999**, *18*, 4563. (k) Puerta, M. C.; Valerga, P. *Coord. Chem. Rev*. **1999**, *193-195*, 977.
2. (a) Chaloner, P. A.; Esteruelas, M. A.; Joó, F.; Oro, L. A.; Homogeneous Hydrogenation; Kluwer, Academic Publishers: Dordrecht, The Netherlands, 1994. (b) Esteruelas, M. A.; Oro, L. A. *Chem. Rev*. **1998**, *98*, 577.
3. Marciniec, B.; Gulinsky, J.; Urbaniak, W.; Kornetka, Z.W. *Comprehensive Handbook on Hydrosilylation*; Marciniec, B. Ed.; Pergamon: Oxford, U. K., 1992.
4. Bruneau, C.; Dixneuf, P. H. *Acc. Chem. Res*. **1999**, *32*, 311.
5. (a) Simionescu, C. I.; Percec, V. *Prog. Polym. Sci*. **1982**, *8*, 133. (b) Masuda, T.; Higashimura, T. *Acc. Chem. Res*. **1984**, *17*, 51. (c) Katz, T. J.; Haker, S. M.; Kendrick, R. D.; Yannoni, C. S. *J. Am. Chem. Soc*. **1985**, *107*, 2182. (d) Szymanska-Buzar, T.; Glowiak, T. *Polyhedron* **1998**, *17*, 3419. (e) Szymanska-Buzar, T.; Glowiak, T. *J. Organomet. Chem*. **1999**, *575*, 98. (f) Szymanska-Buzar, T.; Glowiak, T. *J. Organomet. Chem*. **1999**, *585*, 215.
6. Schrock, R. R. *Acc. Chem. Res*. **1986**, *19*, 342.
7. (a) Trost, B. M.; Flygare, J. A. *J. Am. Chem. Soc*. **1992**, *114*, 5476. (b) Trost, B. M.; Kulawiec, R. J. *J. Am. Chem. Soc*. **1992**, *114*, 5579. (c) Trost, B. M. Martínez, J. A.; Kulawiec, R. J.; Indolese, A. F. *J. Am. Chem. Soc*. **1993**, *115*, 10402. (d) Trost, B. M.; Vidal, B.; Thommen, M. *Chem. Eur. J*. **1999**, *5*, 1055.
8. Trost, B. M.; Pinkerton, A. B. *J. Am. Chem*. **1999**, *121*, 1988.
9. Trost, B. M.; Indolese, A. *J. Am. Chem. Soc*. **1993**, *115*, 8831.
10. (a) Trost, B. M.; Imi, K.; Indolese, A. F. *J. Am. Chem. Soc*. **1993**, *115*, 8831. (b) Trost, B. M. *Chem. Ber*. **1996**, *129*, 1313.
11. Yi, C. S.; Liu, N. *Organometallics* **1998**, *17*, 3158.
12. Trost, B. M.; Toste, D. *J. Am. Chem. Soc*. **1999**, *12*, 9728.
13. Müller, T. E.; Beller, M. *Chem. Rev*. **1998**, *98*, 675.

14. (a) Vollhardt, K. P. C. *J. Org. Chem*. **1984**, *59*, 1574. (b) Brummond, K. M.; Kent, J. L. *Tetrahedron* **2000**, *56*, 3263.
15. Liebeskind, L. S.; Jewell, Jr., C. F. *J. Organomet. Chem*. **1985**, *285*, 305.
16. (a) Dotz, K. H. *Angew. Chem. Int. Ed. Engl*. **1984**, *23*, 587. (b) Wulf, W. D.; Gilbertson, S. R.; Springer, J. P. *J. Am. Chem. Soc*. **1986**, *108*, 520.
17. (a) Miralles-Sabater, J.; Merchán, M.; Nebot-Gil, I.; Viruela-Martín, P .M. *J. Phys. Chem.* **1988**, *92*, 4853. (b) Sodupe, M.; Bauschlicher, G. W. *J. Phys. Chem.* **1991**, *95*, 8640. (c) Sodupe, M.; Bauschlicher, Jr., G. W.; Langhoff, S. R.; Partridge, H. *J. Phys. Chem.* **1992**, *96*, 2118. (d) Mitchell, S. A.; Blitz, M. A.; Fournier, R. *Can. J. Chem*. **1994**, *72*, 587. (e) Böhme, M; Wagener, T.; Frenking, G. *J. Organomet. Chem.* **1996**, *520*, 31.
18. Sellers, H. *J. Phys. Chem*. **1990**, *94*, 8329.
19. (a) Kitaura, K.; Sakaki, S.; Morokuma, K. *Inorg. Chem*, **1981**, *20*, 2292. (b) Ziegler, T. *Inorg. Chem*. **1985**, *24*, 1547. (c) Nielson, A. J.; Boyd, P. D. W.; Clark, G. R.; Hunt, T. A.; Metson, J. B.; Rickard, C. E. F.; Schwerdtfeger, P. *Polyhedron* **1992**, *11*, 1419. (d) Stegmann, R.; Neuhaus, A.; Frenking, G. *J. Am. Chem. Soc.* **1993**, *115*, 11930. (e) Pidun, U.; Frenking, G. *Organometallics* **1995**, *14*, 5325. (f) Li, J.; Schreckenbach, G.; Ziegler, T. *Inorg. Chem.* **1995**, *34*, 3245. (g) Pidun, U.; Frenking, G. *J. Organomet. Chem.* **1996**, *525*, 269. (h) Frenking, G.; Pidun, U. *J. Chem. Soc., Dalton Trans* **1997**, 1653. (i) Hyla-Kriyspin, I.; Koch, J.; Gleiter, R.; Klettke, T.; Walther, D. *Organometallics*, **1998**, *17*, 4724. (j) Decker, S. A.; Klobukowski, M. *J. Am. Chem. Soc.* **1998**, *120*, 9342. (k) Kovács, A.; Frenking, G. *Organometallics* **1999**, *18*, 887.
20. Frenking, G.; Fröhlich, N. *Chem. Rev.* **2000**, *100*, 717.
21. (a) Templeton, J. L. *Adv. Organomet. Chem*. **1989**, *29*, 1. (b) Baker, P. B. *Adv. Organomet. Chem*. **1996**, *40*, 45.
22. (a) Frohnapfel, D. S.; Reinartz, S., White, P. S.; Templeton, J. L. *Organometallics* **1998**, *17*, 3759. (b) Frohnapfel, D. S.; Enriquez, A. E.; Templeton, J. L. *Organometallics* **2000**, *19*, 221.
23. See for example: (a) Tate, D. P.; Augl, J. M. *J. Am. Chem. Soc*. **1963**, *85*, 2174. (b) Wink, D. J.; Creagan, T. *Organometallics* **1990**, *9*, 328. (c) Szymanska-Buzar, T.; Glowiak, T. *J. Organomet. Chem*. **1994**, *467*, 233. (d) Yeh, W.-Y.; Ting, C.-S. *Organometallics* **1995**, *14*, 1417. (e) Mealli, C.; Masi, D.; Galindo, A.; Pastor, A. *J. Organomet. Chem*. **1998**, *569*, 21.
24. See for example: (a) Dötz, K. H.; Müklemeier, J. *Angew. Chem. Int. Ed. Engl.* **1982**, *21*, 929. (b) Salt, J. E.; Girolami, G. J. Wilkinson, G., Motevolli, M.; Thornton-Pett, M.; Hurthouse, M. B. *J. Chem. Soc., Dalton Trans*. **1985**, *685*. (c) Wink, D. J.; Fox, J. R.; Cooper, J. *J. Am. Chem. Soc*. **1985**, *107*, 5012.

25. (a) Wink, D. J.; Creagan, T. *J. Am. Chem. Soc*. **1990**, *112*, 8585. (b) Ishiro, H. ; Kuwata, S.; Ishii, Y.; Hidai, M. *Organometallics* **2001**, *20*, 13.
26. Atwood, J. D. Inorganic and Organometallic Reaction Mechanisms; VCH: New York, 1997; Chapter 3.
27. (a) Esteruelas, M. A.; Gómez, A. V.; López, A. M.; Oro, L. A. *Organometallics* **1996**, *15*, 878. (b) Crochet, P.; Esteruelas, M. A.; López, A. M.; Ruiz, N.; Tolosa, J. I. *Organometallics* **1998**, *17*, 3479. (c) Crochet, P. Esteruelas, M. A.; Gutiérrez-Puebla, E. *Organometallics* **1998**, *17*, 3141. (d) Baya, M.; Crochet, P.; Esteruelas, M. A.; Gutiérrez-Puebla, E.; López, A. M.; Oñate, E.; Tolosa, J.I. *Organometallics* **2000**, *19*, 275. (f) Baya, M.; Crochet, P.; Esteruelas, M. A.; Gutiérrez-Puebla, E.; López, A. M.; Modrego, J.; Oñate, E.; Vela N. *Organometallics* **2000**, *19*, 2585. (g) Esteruelas, M. A.; López, A. M.; Tolosa, J. I.; Vela N. *Organometallics* **2000**, *19*, 4650. (h) Baya, M.; Crochet, P.; Esteruelas, M. A.; Oñate, E. *Organometallics* **2001**, *20*, 240.
28. Esteruelas, M. A.; López, A. M.; Ruiz, N.; Tolosa, J. I. *Organometallics* **1997**, *16*, 4657.
29. Frohnapfel, D. S.; Templeton, J. L. *Coord. Chem. Rev*. **2000**, *206-207*, 199.
30. Templetom, J. L.; Ward, B. C. *J. Am. Chem. Soc*. **1980**, *102*, 3288.
31. Allen, F. H.; Kennard, O.; Watson, D. G.; Brammer, L.; Orpen, A. G.; Taylor, R. *J. Chem. Soc. Perkin Trans*. **1987**, S1.
32. This chemical shift was erroneously reported at 122.9 ppm in reference 27b.
33. Albright, T. A.; Burdett, J. K.; Whangbo, M. H. *Orbital Interactions in Chemistry*; Wiley: New York, 1985.
34. (a) Schilling, B. E. R.; Hoffmann, R.; Faller, J. W. *J. Am. Chem. Soc.* **1979**, *101*, 585. (b) Schilling, B. E. R.; Hoffmann, R.; Faller, J. W. *J. Am. Chem. Soc.* **1979**, *101*, 592.
35. Tatsumi, K.; Hoffmann, R.; Templeton, J. L. *Inorg. Chem.* **1982**, *21*, 466.
36. Orpen, A. G.; Brammer, L.; Allen, F. H.; Kennard, O.; Watson, D. G.; Taylor, R. *J. Chem. Soc. Perkin Trans.* **1989**, S1.
37. (a) Dewar, M. J. S. *Bull. Soc. Chim. Fr.* **1951**, *18*, C79. (b) Chatt, J.; Duncanson, L. A. *J. Am. Chem. Soc.* **1953**, 2939.
38. Shreckenbach, G.; Ziegler, T. *J. Phys. Chem.* **1995**, *99*, 606.
39. (a) Bader, R. F. W. *Atoms in Molecules: A Quantum Theory*, Clarendon Press: Oxford, U.K., 1990. (b) Bader, R. F. W. *Chem. Rev.* **1992**, *92*, 893.
40. Frisch, M. J.; Trucks, G. W.; Schlegel, H. B.; Scuseria, G. E.; Robb, M. A.; Cheeseman, J. R.; Zakrzewski, V. G.; Montgomery, J. A. Jr.; Stratmann, R. E.; Burant, J. C.; Dapprich, S.; Millam, J. M.; Daniels, A. D.; Kudin, K. N.; Strain, M. C.; Farkas, O.; Tomasi, J.; Barone, V.; Cossi, M.; Cammi, R.; Mennucci, B.; Pomelli, C.; Adamo, C.; Clifford, S.; Ochterski, J.; Petersson, G. A.; Ayala, P. Y.;

Cui, Q.; Morokuma, K.; Malick, D. K.; Rabuck, A. D.; Raghavachari, K.; Foresman, J. B.; Cioslowski, J.; Ortiz, J. V.; Stefanov, B. B.; Liu, G.; Liashenko, A.; Piskorz, P.; Komaromi, I.; Gomperts, R.; Martin, R. L.; Fox, D. J.; Keith, T.; Al-Laham, M. A.; Peng, C. Y.; Nanayakkara, A.; Gonzalez, C.; Challacombe, M.; Gill, P. M. W.; Johnson, B.; Chen, W.; Wong, M. W.; Andres, J. L.; Gonzalez, C.; Head-Gordon, M.; Replogle, E. S.; Pople, J. A. Gaussian, Inc., Pittsburgh PA, **1998**.

41. (a) Parr, R. G.; Yang, W. *Density Functional Theory of Atoms and Molecules*; Oxford University Press: Oxford, U. K. **1989**. (b) Ziegler, T. *Chem. Rev.* **1991**, *91*, 651.
42. (a) Lee, C.; Yang, W.; Parr, R. G. *Phys. Rev. B* **1988**, *37*, 785. (b) Becke, A. D. *J. Chem. Phys.* **1993**, *98*, 5648. (c) Stephens, P. J.; Devlin, F. J.; Chabalowski, C. F.; Frisch, M. J. *J. Phys. Chem.* **1994**, *98*, 11623.
43. Hay, P. J.; Wadt, W. R. *J. Chem. Phys.* **1985**, *82*, 299.
44. (a) Francl, M. M.; Pietro, W. J.; Hehre, W. J.; Binkley, J. S.; Gordon, M. S.; Defrees, D. J.; Pople, J. A. *J. Chem. Phys.* **1982**, *77*, 3654. (b) Hehre, W. J.; Ditchfield, R.; Pople, J. A. *J. Chem. Phys.* **1972**, *56*, 2257. (c) Hariharan, P. C.; Pople, J. A. *Theoret. Chim. Acta* **1973**, *28*, 213.
45. Peng, C.; Ayala, P. Y.; Schlegel, H. B.; Frisch, M. J. *J. Comput. Chem.* **1996**, *17*, 49.
46. Reed, A. E.; Curtiss, L. A.; Weinhold, F. *Chem. Rev.* **1988**, *88*, 899.
47. This program was developed by Jose Carlos Ortiz and Carles Bo, Universitat Rovira i Virgili, Tarragona, Spain.